BEHAVIOUR OF COLD-FORMED COMPOSITE BEAM WITH BENT-UP BAR AS SHEAR CONNECTOR ENCASED WITH SELF-COMPACTING CONCRETE

MUSAB NIMIR ALI SALIH

A thesis submitted in fulfilment of the
requirements for the award of the degree of
Doctor of Philosophy

School of Civil Engineering
Faculty of Engineering
Universiti Teknologi Malaysia

AUGUST 2020

DEDICATION

I would like to dedicate all the time spent, knowledge, hard work, and effort on this work sincerely to **ALLAH** and pray for it to be accepted. This work is dedicated to my **father** "A father is neither an anchor to hold us back nor a sail to take us there but a guiding light whose love shows us the way". It is also dedicated to my **mother** and to her I say, "All that I am, or hope to be, I owe to you my angel". To my siblings Dr. Abazer and my sister Dr. Razan for they are my support and to them my everlasting gratitude.

"Strive always to excel in virtue and truth." Prophet Muhammad (peace be upon him)

"No two things have been combined better than knowledge and patience." Prophet Muhammad (peace be upon him)

"The price of success is hard work, dedication to the job at hand, and the determination that whether we win or lose, we have applied the best of ourselves to the task at hand" Vince Lombardi

ACKNOWLEDGEMENT

First and foremost, I would like to express my deepest gratitude to my supervisors Professor Mahmood Md Tahir for his excellent guidance, patient, understanding and valuable advice throughout this research project. I deeply appreciate my co-supervisors Associate Professor Dr. Yusof and Professor Shahrin for their genuine interest, guidance, advices and motivation towards the advancement of my work, without which this work could not have been accomplished.

My sincere appreciation is extended to Dr. Shek for his dedication and commitment as well as the rest of my research group Dr. Firdaus, Eng. Khadavi, Eng. Bram and Eng. Zamzam for their contribution towards my understanding and thoughts.

I am also indebted to the technical staff of Structures and Materials Laboratory, School of Civil Engineering, Universiti Teknologi Malaysia (UTM) for their help rendered during the experimental laboratory works.

The same goes to my friends for their prayers during the research period. should also be recognised for their support. My sincere appreciation also extends to all my colleagues and others who have provided assistance at various occasions. Their views and tips are useful indeed.

ABSTRACT

Composite construction is well-known to be an economical solution by utilizing composite action developed between steel and concrete which has resulted in significant savings in steel weight and reduction in overall beam depth. The advantages of composite construction have contributed to the dominance of multi-storey buildings for medium-rise construction in some countries. However, the use of composite beam with cold-formed steel (CFS) lipped channel section is yet to be established as the structural behaviour of such beam is not well understood. Therefore, this study presents and discusses the behaviour of composite beam proposed for cold-formed steel section attached to profiled metal decking slab with an innovative shear connector. The composite beam comprises of a profiled deck slab arranged perpendicular to two CFS lipped channel sections acting as beam members infilled with self-compacting concrete (SCC), and a U-shaped ribbed rebar as shear connector. The study comprised of two components: experimental and theoretical works. The experimental work consists of fourteen full-scale specimens of the same dimensions (4300 mm x 1500 mm) which were prepared and tested for four-point bending test to investigate the structural behaviour and failure modes of the proposed composite beam system. The specimens are varied based on beam depth (250/150 mm), reinforcement ratio (2.5/1.9), size of shear connector (16/12 mm diameter), beam configuration (back-to-back/toe-to-toe) and types of slab (composite/solid) to study the influences on the ultimate load capacity of the composite specimens. The results showed that slab type, beam configuration, shear connector size and beam depth have significant influences on the ultimate load capacity. Changing from solid slab to composite slab could save about 25% of concrete volume. However, this change could also result in reduction of the ultimate moment resistance (34.1%) based on beam configuration. The results also show that the effective area ratio reduced with an increase in the beam depth. It was noted from all parameters that beam configuration has greater influences on the ultimate moment resistance. Parameter such as back-to-back arrangement has recorded higher increment ranging from 23.3-42.8%. In all specimens, shear connector of size 12 mm proven to be the optimum design configuration and provides a preferable flexible failure mode as compared to concrete brittle failure of shear connector size 16mm. It can be concluded that the proposed composite beam with cold-formed steel section is strong enough to be used as main beam. From the comparison between the experimental result and theoretical prediction using conventional method in EC4. It is found out that the conventional method was not able to predict the ultimate capacity of this composite beam. Hence, a modification had been made to the existing formula. Close agreement is recorded between experimental result and the proposed theoretical model in calculating the ultimate moment resistance of the proposed composite beam.

ABSTRAK

Pembinaan komposit telah terkenal sebagai pemilihan yang kos efektif hasil daripada tindakan komposit antara keluli dan konkrit yang mana dapat mengurangkan kedalaman rasuk dan memberi penjimatan ketara ke atas berat sendiri keluli. Kelebihan yang ada pada pembinaan komposit telah menyumbang kepada dominasi dalam pembinaan bangunan keluli bertingkat separa tinggi di beberapa negara. Walau bagaimanapun, penggunaan rasuk komposit dengan keluli tergelek sejuk (CFS) dalam bentuk C masih belum diguna pakai kerana kelakuan struktur rasuk tersebut tidak difahami dengan baik. Oleh itu, kajian ini membentangkan kelakuan rasuk komposit menggunakan keratan keluli tergelek sejuk dan digabungkan dengan papak komposit yang inovatif. Rasuk komposit terdiri daripada papak komposit yang disusun serenjang ke atas dua keratan CFS berbentuk C yang bertindak sebagai anggota rasuk yang dipenuhi dengan konkrit berupaya mampat sendiri (SCC), dan tetulang keluli berbentuk U sebagai penyambung ricih. Kajian ini terdiri daripada dua komponen: kerja eksperimen dan analisa teori. Kerja eksperimen merangkumi empat belas rasuk komposit berskala penuh dengan dimensi yang sama (4300 mm x 1500 mm) dan diuji bawah ujian lenturan empat titik bagi mengkaji tingkah laku struktur dan mod kegagalan sistem rasuk komposit. Spesimen-spesimen ini adalah berbeza mengikut kedalaman rasuk (250 / 150 mm), nisbah tetulang (2.5 / 1.9), saiz penyambung ricih (garis pusat 16 / 12 mm), konfigurasi sususan rasuk (back-to-back / toe-to-toe) dan jenis papak (komposit / pepejal) untuk mengkaji pengaruh ke atas rintangan beban muktamad rasuk komposit. Keputusan menunjukkan bahawa jenis slab, konfigurasi rasuk, saiz penyambung ricih dan kedalaman rasuk mempengaruhi rintangan beban muktamad. Perubahan dari papak padu ke papak komposit dapat menjimatkan 25% jumlah kuantiti konkrit. Walaubagaimanapun, perubahan ini juga mengakibatkan pengurangan rintangan lenturan muktamad (34.1%) berdasarkan konfigurasi rasuk. Keputusan juga menunjukkan bahawa nisbah luas berkesan berkurangan dengan peningkatan kedalaman rasuk. Daripada semua parameter, konfigurasi rasuk memberi pengaruh ketara ke atas rintangan lenturan muktamad rasuk komposit. Parameter seperti susunan CFS secara back-to-back telah mencatatkan peningkatan yang lebih tinggi iaitu dalam julat 23.3-42.8%. Dalam semua spesimen, saiz penyambung ricih 12 mm adalah konfigurasi reka bentuk paling optimum dan memberikan kegagalan fleksibel yang lebih baik berbanding dengan kegagalan konkrit bagi saiz penyambung ricih 16 mm. Boleh disimpulkan bahawa rasuk komposit yang dicadangkan dengan keratan keluli tergelek sejuk adalah sesuai untuk digunakan sebagai rasuk utama. Daripada perbandingan antara keputusan eksperimen dan analisa teori menggunakan kaedah dalam kod amalan EC4, didapati bahawa kaedah konvensional tidak dapat menganggarkan rintangan lenturan muktamad rasuk komposit ini. Oleh itu, pengubahsuaian telah dibuat ke atas kaedah yang sedia ada. Kesetaraan telah dicapai antara keputusan eksperimen dan kaedah teori yang diubahsuai dalam mengira rintangan lenturan muktamad rasuk komposit yang dicadangkan.

TABLE OF CONTENTS

LIST OF TABLES

LIST OF FIGURES

LIST OF ABBREVIATIONS

CFS	-	Cold-Formed Steel
SCC	-	Self-Compacting Concrete
CBS	-	Composite Beam Specimen
TT	-	Toe-to-toe (box-section)
BB	-	Back-to-back (I-section)
SS	-	Solid Slab
$H-Slip$	-	Horizontal Slip
MPD	-	Midpoint Deflection
LPD	-	Loading Point Deflection
COV	-	Coefficient of Variation
LVDT	-	Linear Variable Displacement Transducer
ACI	-	American Concrete Institute
AISC	-	American Institute of Steel Construction
BS	-	British Standard
EC2	-	Eurocode 2
EC3	-	Eurocode 3
EC4	-	Eurocode 4
FEM	-	Finite Element Modelling
HRS	-	Hot Rolled Steel
NA	-	Neutral Axis
RC	-	Reinforced Concrete
NRC	-	Normal Reinforced Concrete
NVC	-	Normal Volume Concrete
SG	-	Strain Gauge
SF	-	Slump Flow
SP	-	Superplasticizer
VMA	-	Viscosity Modifying Admixtures
AASHTO	-	American Association of State Highway and Transportation Officials

LIST OF SYMBOLS

A_g	-	Gross cross-sectional area with sharp corners
$A_{g,rounded}$	-	Gross cross-sectional area with rounded corners
A_{eff}	-	Effective area
A_v	-	Shear area of steel
A_a	-	Cross-sectional area of steel beam
A_s	-	Area of steel
A_r	-	Area of reinforcement
A_{st}	-	Area of stiffeners
b_{eff}	-	Concrete slab effective width
b	-	Beam width
b_{p1} and b_{p2}	-	Notional width of Flange in compression and Tension respectively
b_f	-	Steel flange width
b_{e1} and b_{e2}	-	Effective flange width
b_c	-	Width of cut in steel flange
b_s	-	Width of shear connector
c	-	Edge fold
c_p	-	Notional edge fold
C_1 and C_2	-	Coefficients depending on the loading and end restraint conditions
c_{eff}	-	Effective width of the edge fold
d	-	Diameter of rebar
d'	-	Concrete cover
E_s	-	Modulus of elasticity of steel
E_c	-	Modulus of elasticity of concrete
f_y	-	Yield Stress

f_{yb}	-	Basic Yield Stress
f_u	-	Ultimate stress
f_{ck}	-	Concrete cylinder compressive strength
f_{cu}	-	Concrete cube compressive strength
f_{cd}	-	Design compressive strength
f_{yr}	-	Yield strength of reinforcement
f_{yst}	-	Yield strength of stiffeners
f_{bv}	-	Shear buckling strength
F_s	-	Resistance of steel
F_r	-	Resistance of reinforcement
F_{st}	-	Resistance of stiffeners
G	-	Shear modulus
h	-	Height of beam
h_{eff}	-	Effective compression zone in web
h_c	-	Depth of concrete slab
h_p	-	Depth of profiled steel sheeting rib
h_{e1} and h_{e2}	-	Effective web height
h_{sc}	-	Height of shear connector
h_w	-	Height of web between the mid-lines of flanges
h_s	-	Height of shear connector
I_z	-	Second moment of area about the minor axis
I_w	-	warping constant
I_t	-	torsion constant
I_{eff} or $I_{eff,y}$	-	Effective second moment of area
k_t	-	Factor taking the effect of the steel decking
k_w	-	Effective length factors
k	-	Flexural stiffness

k_{100}	-	Flexural stiffness at 100 kN
k_{τ}	-	Shear buckling coefficient taken as 5.34
k_{σ}	-	Buckling factor
K_{nom}	-	Normalized stiffness
L	-	Beam length between points which have lateral restraint
M_{u}	-	Section ultimate moment
M_{cr}	-	Elastic critical moment for lateral torsional buckling
$M_{c,Rd}$	-	Design moment resistance of composite specimen with partial shear connection
M_{Ed}	-	Applied bending moment
$M_{f,Rd}$	-	Plastic moment of composite section ignoring the web
$M_{u,\exp}$	-	Experimental ultimate moment
$M_{pI,Rd}$	-	Plastic moment resistance of the fully composite beam
M_{Rd}	-	Theoretical ultimate moment
$M_{b,Rd}$	-	Buckling Moment in steel element
$M_{pI,steel}$	-	Moment resistance of the CFS beam
$N.A$	-	Neutral axis
n	-	Number of shear connectors
P_{e}	-	Elastic load
P_{u}	-	Ultimate load
$P_{y.loading}$	-	Yield load at loading point
$P_{y.center}$	-	Yield load at centre point
$P_{Rd,s}$	-	Shear design resistance of shear connector
$P_{Rd,c}$	-	Shear design resistance of concrete
R	-	Design element resistance
R_{c}	-	Resistance of concrete element
R_{s}	-	Resistance of steel element
R_{w}	-	Resistance of web crippling

R_Q	-	Total shear force transferred by shear connectors
r	-	Corner radius
S_u	-	Slip at ultimate load
S_e	-	Slip at elastic load
t	-	Thickness
t_f	-	Thickness of flange
t_w	-	Thickness of web
t_{nom}	-	Nominal thickness
υ	-	Poisson's ratio
V_{Rd}	-	Design shear resistance
$V_{b,Rd}$	-	Buckling Shear resistance of the CFS section
$V_{pI,Rd}$	-	Plastic Shear resistance of the CFS section
V_{Ed}	-	Applied vertical shear force
$V_{u,\exp}$	-	Experimental shear
$W_{eff,y,c}$	-	Effective section modulus in compression
$W_{eff,y,t}$	-	Effective section modulus in tension
W_{eff}	-	Design effective section modulus
x	-	Depth of the neutral axis from the top fibre
y_p	-	Depth of steel in compression
Z_g	-	Distance between the point of load application and the shear centre
Z_c	-	Distance from the neutral axis to maximum compression fibre
Z_t	-	Distance from the neutral axis to maximum tension fibre
α	-	Shear connector height to diameter ratio
α_{LT}	-	Imperfection factor
$\sigma_{0.2}$	-	Yield stress using offset method
$\sigma_{\max}$	-	Maximum applied stress
δ_u	-	Deflection at ultimate load

δ	-	Factor considering the rounded corner effect
ρ	-	Reinforcement ratio
ϕ	-	Slope of the web relative to the flanges
ϕ_{LT}	-	lateral torsional buckling factor
χ_d	-	Reduction factor
χ_{LT}	-	Reduction factor of lateral torsional buckling
γ_{mo}	-	Partial safety factor
γ_{m1}	-	Partial safety factor
γ_a	-	Partial safety factor for Steel taken as 1.05
γ_v	-	Partial safety factor for shear connector taken as 1.25
γ_c	-	Partial safety factor for concrete taken as 1.50
λ_{LT}	-	Non-dimensional slenderness factor
λ_w	-	Web slenderness
τ_{ba}	-	Simple post-critic resistance
η	-	Degree of shear connection
η_{EC}	-	Degree of shear connection using EC4
η_p	-	Degree of shear connection using proposed method
ψ	-	Stress ratio

LIST OF APPENDICES

CHAPTER 1

INTRODUCTION

1.1 Background

Today, there is an ever-increasing effort to improve building construction efficiency, using innovative building construction methods to reduce time and cost. In steel construction, there are two main types of structural members. One is the familiar group of hot-rolled steel (HRS) and component members of built-up sections from plates usually meant for heavy loading structures. The other, a less familiar but of growing importance, is thin sections known as cold-formed steel (CFS) section usually or also known as light-weight structures. However, the latter method of construction is getting popular in our present era of building constructions Irwan, (2011). In the mid-20th century, the structural use of CFS sections was further extended for commercial and industrial building constructions Hancock et al., (2001); Riley and Cotgrave, (2014). Recently, the use of CFS sections as a construction material is not only limited to roof structure but also as wall panelling and floor slab as the strength and the capacity of the sections have been improved due to the quality assurance of manufacturing and method of construction (Yu, 2019).

Hot-rolled steel sections are formed under high temperatures up to 1400℃ in a blast furnace or electric arc furnace, while the CFS sections are manufactured at room temperature. The difference of the manufacturing process makes the properties be of hot-rolled and CFS disparity in strength, structural performance, and failure mode. The typical thickness of the CFS section is ranged from 0.9mm to 4mm. CFS is usually galvanized to protect the members from corrosion which increases its corrosion protection. In the forming process, due to cold working by the process of strain hardening, the yield strength of the steel tends to increase. There are three methods to manufacture the CFS sections: cold roll forming, press braking, and bending brake operation. Among them, cold roll forming and press breaking as in Figure 1.1 is widely

used to produce building components (structural members, roof truss, wall panel, frames of windows and doors, etc.).

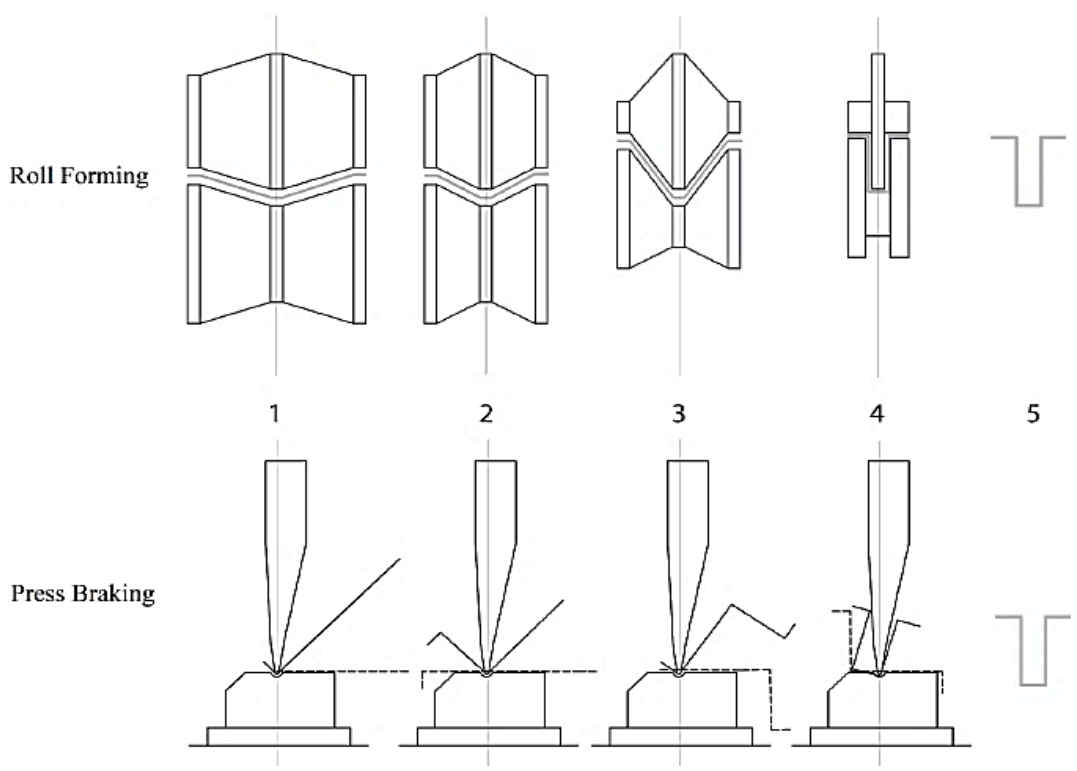

Figure 1.1 The forming methods of cold-formed steel

In the past, CFS sections were used as secondary structural members, for example, roof purlin and side rail for wall cladding. The thin-walled section tends to limit the structural performance of CFS sections by premature buckling and instability. Over the past two decades, the increasing applications of CFS in the construction industry have brought to more innovative researches in progress Lau and Hancock, (1987); LaBoube, (1993); Rogers and Hancock (1997); Wilkinson and Hancock (2000); El-Kassas, Mackie et al., (2002); Schafer, (2002); Holesapple and LaBoube (2003); Stephens and LaBoube, (2003); Yu and Schafer, (2003); Young, (2004); Young and Ellobody, (2005); Guzelbey, Cevik et al., (2006); Yu and Schafer, (2006); LaBoube and Findlay, (2007); Dubina, (2008); Pala, (2008); Ranawaka and Mahendran, (2009); Kumar and Kalyanaraman, (2012); Macdonald and Heiyantuduwa, (2012) to ensure the stability and reliability of the constructed steel structures. As the industry demand grows gradually, many research studies were done to minimize the safety issue and exhilarated the use of CFS members as primary

structural members. However, the main limiting features of CFS are the thinness of the section that makes it susceptible to torsional, distortional, lateral-torsional, lateral-distortional and local buckling problems Irwan, et al., (2011) and its inability to be welded. The structural behaviour and performance of such thin-walled, cold-formed structural members under loads differ in several significant respects from that of heavy hot-rolled steel sections. As a result, design specifications for heavy hot-rolled steel construction cannot possibly cover the design features of CFS construction completely. The current codes of practice cover the design considerations for plain CFS members subjected to compression, tension, bending, shear or combinations. However, the use of CFS members in composite with concrete is still very limited. This is due to the fact that no standard specifications have been established for CFS sections as composite members.

The thinness of the CFS section which is classified as slender section makes it susceptible to torsion, distortional, lateral torsion, lateral distortional and local buckling Irwan et al, (2011) resulted in the profile failed before reaching its yield strength. The resistance of CFS sections to such instability problems could be well improved by using the composite construction method. The composite action of CFS should be integrated together with concrete to form into a composite beam system by means of a shear connector. Therefore, two CFS lipped channel sections arranged back-to-back to form an I-section or arranged as toe-to-toe to form a box-section filled with concrete to form composite beams. These proposed composite beams are then connected to the slab by re-bars bent into U-shape as shear connectors. The proposed system of these composite construction should be able to form into symmetric sections and increase significantly lateral-torsional resistance and pre-mature failure due to the thinness of the section. Thus, the potential of buckling at the CFS section could be prevented as well as producing prefabricated construction and more robust. These two advantages possess by the system, promote the use of CFS sections in a wider range of structural applications Irwan, et al., (2009); Irwan, et al., (2011); Lawan et al., (2015); Alhajri et al., (2016); Bamaga et al., (2019). Since the governing failure mode of CFS thin-walled elements is buckling (either local, distortional or global), intensive experimental research was carried out on the effect of secondary structures, which can significantly increase the capacity of the CFS designed as composite construction.

Composite construction has become a popular method in recent years and has largely accounted for the dominance of steel frames in many countries. Composite steel-concrete beams are widely used due to savings in steel weight, higher stiffness, longer spans, and rapid erection, etc.; some of the advantages of construction. A composite floor system conventionally consists of a reinforced concrete slab that is supported on a set of steel joists. Steel and concrete parts should be fully connected such that shear flow can be transferred between them. The composite integrity is provided by shear connectors. The basic idea in composite construction is to use the advantages of both steel and concrete materials while avoiding their inherent disadvantages. The ability of composite slab to carry the loads depends on the degree of shear connectors provided between the concrete and the steel. Therefore, whenever the interaction between these two materials increased, the capacity, stiffness, and efficiency of the composite slab also increased. In order for composite action to be integrated between steel and concrete, shear connectors should be provided so that the tension in steel and the compression in concrete can be fully utilized. A typical steel-concrete composite cross-section in composite beam construction is depicted in Figure 1.2.

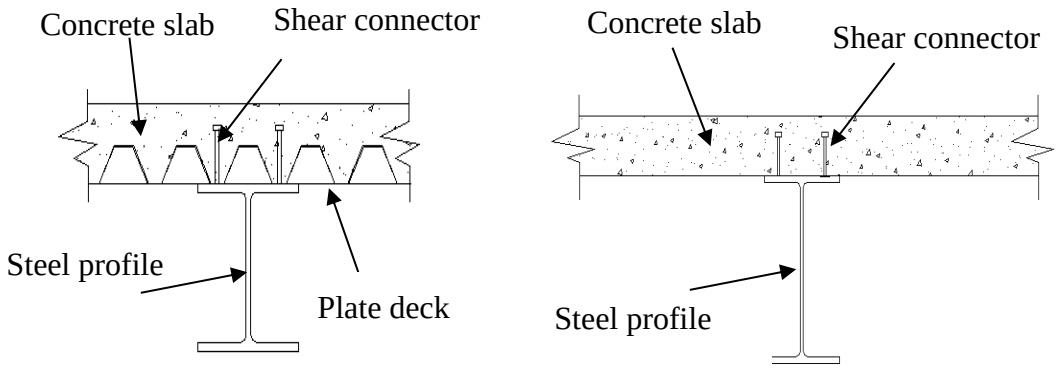

Figure 1.2 Steel-concrete composite cross-section

Composite construction using the CFS section and concrete began in Europe in the mid-1940s was used as a floor system Allen, (2006) and Talal, (2014). Composite action is categorized by an interactive behaviour between structural steel and the concrete designed to utilize the best load resistance capability. Sections are more durable, stiffer and stronger than using single materials, resulting in lower

material cost, with an estimated cost savings of 10–30% in comparison with conventionally fabricated sections and more than 30% compared with standard hot-rolled beams Dan Dubina et al., (2015). For the structural components to act compositely, a mechanical means of the shear connection must be provided Prakash et al., (2012). The most generally used shear connectors are the headed studs shear connectors which are commonly provided at the interface between the concrete and the steel to resist the longitudinal shear (Lim et al., 2013).

Steel is a material that works very well in tension with the plastic stress distribution in the composite slab. The proportions of the concrete slab and steel section refer to that the plastic neutral axis usually lies within the concrete slab. Therefore, all steel is in tension. The concrete material works well in compression but has insignificant resistance to tension. Hence for construction purposes, it conventionally depends on the profiled steel deck to carry the tensile forces (this is the role played by the steel deck as part of the composite cross-section which is also efficient to provide laterally restrained). The steel part of a cross-section undergoes tension, and concrete undergoes the compression force.

The design of shear connectors is a vital aspect in the design of composite beams. Shear connectors can resist the horizontal shear and provide vertical interlocking between the concrete slab and steel beams to produce a composite section that acts as a single unit. For conventional hot-rolled steel composite structures, extensive research has already been carried out to develop the most efficient and commercially viable shear connectors. Welded headed shear studs are most prominently used in conventional composite structures as shear connectors. Due to the thinness of the CFS sections, welding of shear studs is not viable Hanaor, (2000); hence, the development of shear connectors for CFS and concrete composite structures is of utmost importance and require further research.

Therefore, this research investigates the structural performance of CFS with Self-Compacting Concrete (SCC) as a composite beam system, focused on full-scale testing on a new type of composite beam system with CFS connected together to SCC slab by means of an innovative type of shear connector. The proposed composite beam

system is illustrated in Figure 1.3 and detailed in Chapter 3. The structural system components consist of CFS beams comprised of two back-to-back and toe-to-toe C-sections arranged together and connected to a corrugated steel deck as SCC slab (which acts as formwork for the concrete slab). Bent-up deformed rebar is proposed as a shear connector connected to the SCC slab and proposed boxed section as a beam. Self-drilling fasteners are used for connecting all the steel parts. The findings from this study may magnify the use of CFS in the construction method in a composite beam with CFS sections and may also promote the use of the proposed bent-up rebar as shear connection enhancement as an alternative in composite construction for small and medium-size buildings as well as lightweight industrial constructions.

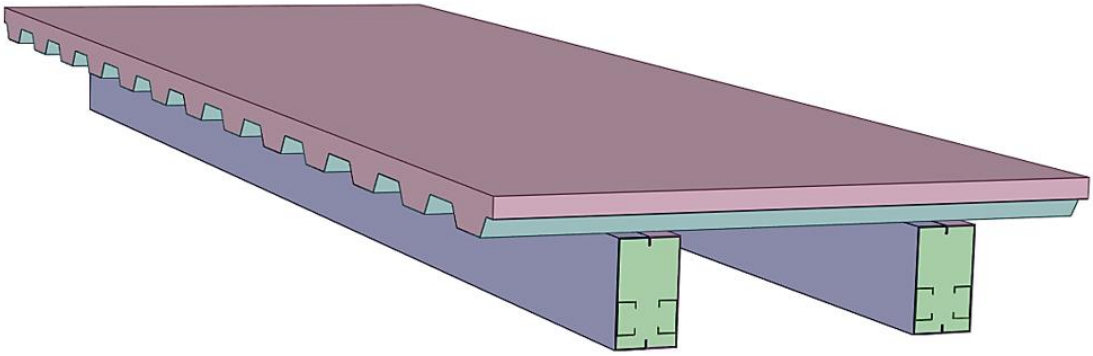

a) Proposed Composite Beam

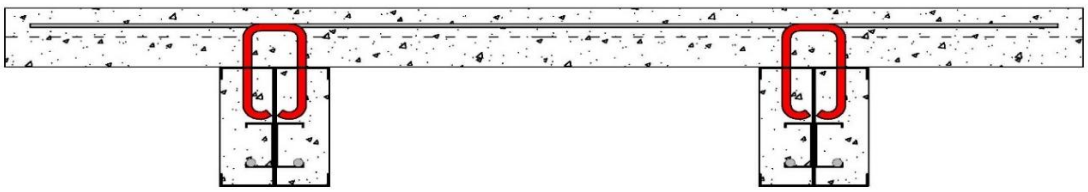

b) Back-to-back composite beam

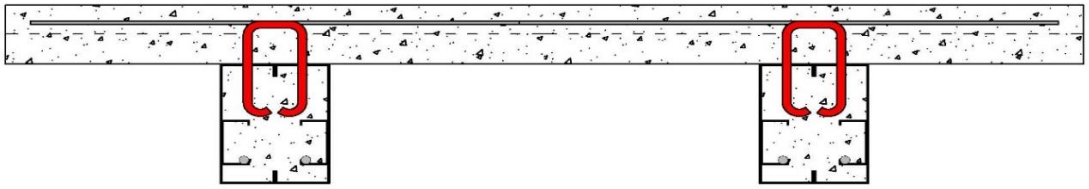

c) Toe-to-toe composite beam

Figure 1.3 Proposed floor system. a) back to back, b) toe-to-toe

1.2 Problem Definition

The use of CFS as construction materials is known to have significant advantages such as lightweight, cost-effective, easy to handle, and environmentally friendly. Such significant advantages, however, could not be fully utilized due to the thin section classified as a slender section. As explained earlier, thin sections tend to fail due to pre-mature failure due to buckling and deformation. The cross-section failed below the elastic stress in bending and compression. However, the main limiting feature of CFS as reported by many researchers Yamaki, (1959); Timoshenko and Gere, (1961); Schafer, (2002); Dubina and Ungureanu, (2002); Yu and Schafer, (2006); Li & Schafer, (2010); Irwan, et al., (2011); Bonada et al., (2018) is the thinness of the section that makes it susceptible to torsional, distortional, lateral-torsional, lateral-distortional, local buckling problems and inability to weld. As a result, composite construction method is proposed so that the strength of the section can be improved. In this study, a new type of composite beam was proposed comprised of partially encased built-up CFS beams with Self-Compacting Concrete (SCC) slab to generate composite action between CFS and SCC slab by means of a new proposed shear connection. The proposed shear connector was developed from a U-shaped bent ribbed re-bar to eliminate the need for welding. The shear connector should be able to increase the surface area and hence enhance the shear connection between steel and concrete. The need for this new shear connector instead of the common headed stud is mainly to solve the problem of thin sections weldability. Therefore, this issue could be studied by partially encasing the CFS with cohesive concrete known as SCC which could be compacted by its own self-weight while its homogeneity is maintained. Tap-screws were used in the formation of a boxed CFS beam to enhance the interaction between the CFS and SCC as well as to eliminate local buckling of CFS. The proposed composite beam section should be able to increase the flexural strength and reduce the deflection of the beam and significantly increase the stiffness of the proposed composite beam system.

The research questions are as follows:

1. How does the composite double beam using double back-to-back and toe-to-toe lipped C-channel profiles behave under bending?

2. Can the proposed configurations of the composite beams be used as an alternative to hot-rolled steel and whether it can be applied to medium level buildings?
3. Is it possible for the proposed bent-up rebar to be used as a shear connector?
4. Can the proposed composite configuration significantly increase the capacity and stiffness of the CFS?

1.3 Objectives Research

The objectives of this study is to investigate the behaviour and performance of a composite beam with partially encased CFS section with SCC slab, using re-bars as shear connectors, to provide composite action and to improve the understanding of the parameters that affect the capacity of the composite beam. The objectives of this research are detailed as follows:

1) To carry out full-scale experiments in order to assess the structural behaviour of the proposed composite beam with partially encased CFS section profiles and SCC slab,

2)To investigate the performance of the bent-up deformed rebar as a shear connector, to be used in the proposed composite beam,

3)To validate the performance of the proposed CFS-SCC composite beam system by comparing with theoretical predictions based on Eurocode 4,

4)To propose a new formulation to predict the moment resistance of the proposed composite beam with CFS.

1.4 Scope of the Study

The scope of this study consists of an experimental investigation and theoretical validation. The experimental program is designed to provide a better understanding of the structural performance of the proposed composite beams. Full-scale tests were conducted to investigate the structural behaviour of the proposed composite beam system comprised of profiled metal decking slab with self-compacting concrete (SCC), integrated together with two parallel CFS built-up beams infilled with SCC by means of U-shaped rebar as shear connectors. A total of fourteen specimens were prepared and tested until failure occurred to get a better understanding of the performance behaviour. All specimens had the same length of 4000 mm from support to support. In addition, the concrete slab in each specimen was 100 mm thick and 1500 mm wide. Full-scale simply supported beam specimens of 4000 mm length between supports are tested using a four-point load system. The beam is subjected to two-point loads in one-fourth of the span (1000 mm from each support). This system of loading produces a constant region of a pure bending moment between the point loads. Hence, the ultimate flexural capacity of the proposed composite beam is determined. A profile metal deck was installed to form the concrete slab that was oriented perpendicular to the steel composite beams. The slab was reinforced by two layers of steel mesh arranged at the top and bottom of the solid slab and one layer at the top of the composite slab which had a nominal cover of 20 mm. The steel mesh (A142) was spaced at 200 mm in both the longitudinal and transverse directions with a diameter of 6 mm.

The proposed composite beam comprises two CFS beams each consists of two cold-formed lipped steel C-sections oriented back-to-back to form an I-section beam or toe-to-toe to form a box-section beam, all beams were infilled with SCC to make a composite beam. Two composite beams were arranged parallel to each other and spaced at 750 mm. Two of these composite beam sections were placed perpendicularly to the profiled metal decking. Two different depths of the CFS box beams were considered: 250 mm and 150 mm. A CFS lipped channel section (C75) was used as a stiffener along with a rebar diameter of size 12 mm, which were installed as longitudinal reinforcements in the infilled CFS composite box sections, size 250 mm.

Only two sample used rebar size 20 instead of C75 as reinforcement. For a beam of size 150 mm, a rebar size of 16 mm in diameter was used as longitudinal reinforcement.

A novel shear connector was used in this research, which was made up of U-shaped bent ribbed rebar, to increase the surface area of the shear connector between the steel and concrete. Two different nominal diameters of the shear connectors were used (size 12 and 16 mm) at a longitudinal spacing of 332 mm. The shear connectors were installed between the slab and the infilled CFS composite beams by making a small cut on the top surface of the CFS beams.

The theoretical validation of the proposed modified equation to predict the strength capacity of proposed shear connectors depending on their mechanism to resist the longitudinal load. A comparison between theoretical values and experimental results is conducted to validate the use of the modified method as well as the current design methods of a composite beam for designing the proposed composite cold-formed steel-concrete beams.

1.5 Significance of the Study

Composite beams are known to be stiff, cost-effective and, material savings and efficiency in strength are widely used in the construction industry (Lee et al., 2014). However, the use is very much popular with the Hot-Rolled Steel Section where a standard shear stud can be welded to the top flange of the steel beam. However, the use with CFS is not that popular as the section is limited due to its thin section and the shear stud cannot be welded to the CFS section. The primary advantages of cold-formed steel are lightweight, high strength and stiffness, ductility, uniform quality, dimensional stability, ease of prefabrication and mass production, economy in transportation and handling can be fully utilized if the sections are designed as composite construction knowing that the conventional shear connectors are not applicable when using CFS due to inability to weld and the CFS susceptibility to buckling due to its thinness, modification to the current method of composite beam

has to be introduced. An innovative shear connector that can be installed without the need to weld has to be adopted in this research. Partially encase the CFS beam with the use of tap-screw in the CFS web in order to enhance the CFS-SCC interaction and therefore delaying or preventing the premature buckling failure of the CFS beams.

Therefore, the validation of using CFS sections with concrete as a composite beam could significantly increase their strength and stiffness capacities Bamaga et al., (2013); Saggaff et al., (2015); Lawan et al., (2015); Bamaga et al., (2019). The concrete slab could provide lateral bracing that prevents the CFS section to fail under lateral-torsional buckling. Also, it could improve the resistance of the top flange and reduce its tendency to buckle under compression. The proposed study in this thesis should be able to provide an alternative construction method in the steel construction industry that provide cheap and easy to handle structural members. The system can also enhance the construction method as one of the Industrialised Building System (IBS) which can be produced in the factory and assemble on-site.

1.6 Thesis Outline

Chapter 1 a brief overview of the manufacture and history of CFS members and composite structures is presented, and the problem was identified. The research objectives and scope are stated, and the thesis outline is presented.

Chapter 2 presents a comprehensive literature review on the composite structures and its components as well as the behaviour or CFS based on experimental, numerical and analytical investigations conducted by previous researchers. Current design methods and material characteristics.

Chapter 3 describes the experimental investigation performed of composite CFS flexural members and composite action, along with the material properties and the test procedure of a built-up CFS with SCC.

Chapter 4 presents and discusses the experimental results of materials properties tests for the materials used in the study. Results and discussion of the experimental investigation as well as their modes of failure are also discussed. Theoretical calculations for the CFS section, validation analysis and calculations of the proposed CFS-SCC composite beams using a modified method in comparison to the current design codes and methods. Comparison between experimental, theoretical and other researches is also conducted.

Chapter 5 Provide Conclusions and Recommendations provides an overview of the developed work and a summary of the most significant findings of this research and presents recommendations for possible future research.

REFERENCES

Abbasi, M., Khezri, M., Rasmussen, K. J. R., & Schafer, B. W. (2018). Elastic buckling analysis of cold-formed steel built-up sections with discrete fasteners using the compound strip method. Thin-Walled Structures, 124, 58-71.

Abdel-Sayed, G. (1982). Composite cold-formed steel-concrete beams. Journal of the Structural Division, 108(11), 2609-2622.

Abdullah, R., & Easterling, W. S. (2009). New evaluation and modeling procedure for horizontal shear bond in composite slabs. Journal of constructional steel research, 65(4), 891-899.

Ahmad, S., Umar, A., & Masood, A. (2017). Properties of normal concrete, self-compacting concrete and glass fibre-reinforced self-compacting concrete: an experimental study. Procedia engineering, 173, 807-813.

Ahn, J. H., Lee, C. G., Won, J. H., & Kim, S. H. (2010). Shear resistance of the perfobond-rib shear connector depending on concrete strength and rib arrangement. Journal of Constructional Steel Research, 66(10), 1295-1307.

AISC, A. (2005). 360-Specification for Structural Steel Buildings; American Institute of Steel Construction.

AISI. (2007). North American Specification for the Design of Cold-Formed Steel Structural Members.

AISI. (2008). AISI STANDARD: Standard Test Method for Determining the Web Crippling Strength of Cold-Formed Steel Beams. Manual on Hydrocarbon Analysis, 6th Edition, 545-545–3. https://doi.org/10.1520/mnl10913m

Alenezi, K., Tahir, M. M., Alhajri, T., Badr, M. R. K., & Mirza, J. (2015). Behaviour of shear connectors in composite column of cold-formed steel with lipped C-channel assembled with ferro-cement jacket. Construction and building materials, 84, 39-45.

Alhajri, T. M., Tahir, M. M., Azimi, M., Mirza, J., Lawan, M. M., Alenezi, K. K., & Ragaee, M. B. (2016). Behaviour of pre-cast U-Shaped Composite Beam integrating cold-formed steel with ferro-cement slab. Thin-Walled Structures, 102, 18-29.

Allen, D. (2006). History of cold formed steel. STRUCTURE magazine, 28-32.

Alves, A. R., Isabel, B. V., Washintgon, B. V., & Gustavo, S. V. (2018). Prospective study on the behaviour of composite beams with an indented shear connector. Journal of Constructional Steel Research, 148, 508-524.

Anderson, N. S., & Meinheit, D. F. (2000). Design criteria for headed stud groups in shear: Part 1-Steel capacity and back edge effects. PCI journal, 45(5), 46-75.

Ardalan, R. B., Joshaghani, A., & Hooton, R. D. (2017). Workability retention and compressive strength of self-compacting concrete incorporating pumice powder and silica fume. Construction and Building Materials, 134, 116-122.

Aslani, F., & Gedeon, R. (2019). Experimental investigation into the properties of self-compacting rubberised concrete incorporating polypropylene and steel fibers. Structural Concrete, 20(1), 267-281.

Asteris, P. G., & Kolovos, K. G. (2019). Self-compacting concrete strength prediction using surrogate models. Neural Computing and Applications, 31(1), 409-424.

ASTM, Q. A792-Specification for Steel Sheet Aluminum Zinc Alloy Coated by the Hot Dip Process. General Requirements.

Bamaga, S. O., Tahir, M. M., & Tan, C. S. (2012). Push tests on innovative shear connector for composite beam with cold-formed steel section.

Bamaga, S. O., Tahir, M. M., Tan, C. S., Shek, P. N., & Aghlara, R. (2019). Push-out tests on three innovative shear connectors for composite cold-formed steel concrete beams. Construction and Building Materials, 223, 288-298.

Bamaga, S. O., Tahir, M. M., Tan, T. C., Mohammad, S., Yahya, N., Saleh, A. L., ... & Rahman, A. B. A. (2013). Feasibility of developing composite action between concrete and cold-formed steel beam. Journal of Central South University, 20(12), 3689-3696.

Bärtschi, R. (2005). Load Bearing Behaviour of Composite Beams in Low Degrees of Partial Shear Connection (Vol. 290).

Bärtschi, R., & Fontana, M. (2004, June). A nonlinear numerical analysis model for composite beams. In Proceedings of the PhD Symposium, Delft University.

Bonilla, J., Bezerra, L. M., & Mirambell, E. (2019). Resistance of stud shear connectors in composite beams using profiled steel sheeting. Engineering Structures, 187, 478-489.

Bonilla, J., Bezerra, L. M., Larrúa Quevedo, R., Recarey Morfa, C. A., & Mirambell Arrizabalaga, E. (2015). Study of stud shear connectors behaviour in composite beams with profiled steel sheeting. Revista de la construcción, 14(3), 47-54.

Boukendakdji, O., Kadri, E. H., & Kenai, S. (2012). Effects of granulated blast furnace slag and superplasticizer type on the fresh properties and compressive strength of self-compacting concrete. Cement and concrete composites, 34(4), 583-590.

Bouziani, T. (2013). Assessment of fresh properties and compressive strength of self-compacting concrete made with different sand types by mixture design modelling approach. Construction and Building Materials, 49, 308-314.

BS EN 1992-1-1. (2004). Eurocode 2: Design of concrete structures - Part 1-1: General rules and rules for buildings. British Standards Institution, 1(2004), 230. https://doi.org/ [Authority: The European Union Per Regulation 305/2011, Directive 98/34/EC, Directive 2004/18/EC]

BS EN 1993-1-1. (2013). Eurocode3: Design of Steel Structures-Part1-1: General rules and rules for buildings (Vol. 1). https://doi.org/10.1017/CBO9781107415324.004

BS EN 1993-1-3. (2012). Eurocode3: Design of cold-formed steel structures-Part 1-3: Design of Cold Formed Steel Structures.

BS EN 1994-1-1. (2012). Designers' guide to Eurocode 4 design of composite steel and concrete structures: EN 1994-1-1, 2nd Edition. https://doi.org/10.1680/dcsb.41738

BS EN 206. (2013). BSI Standards Publication Concrete — Specification, performance, production and conformity. British Standard, (May), 30.

BS EN206 (2010). Concrete-Part 9: Additional Rules for Self-compacting Concrete. London: British Standard Institution.

BS10002-1 (2001). Metallic materials-Tensile Testing-Part 1: Method of test at ambient temperature. London: British Standard Institution.

BS1881 (1983). Testing concrete-Part 116: Method for determination of compressive strength of concrete cubes. London: British Standard Institution.

BS1881 (1983). Testing concrete-Part 121: Method for determination of static modulus of elasticity in compression. London: British Standard Institution.

BS5400 (1979). Steel, concrete and composite bridges-Part 5: Code of practice for design for design of composite bridges. London: British Standard Institution.

BS5950 (2010). Structural use of steelwork in building-Part 3.1: 1990+A1: Design in composite construction-section 3.1 Code of practice for design of simple and continous composite beams. London: British Standard Institution.

BS5950-5. (1998). Structural use of steelwork in building. Part 5 Code of practice for the design of cold-formed sections. Part 5 (Vol. 3). Retrieved from http://www.sefindia.org/forum/files/bs5950_4_156.pdf

Cândido-Martins, J. P. S., Costa-Neves, L. F., & Vellasco, P. D. S. (2010). Experimental evaluation of the structural response of Perfobond shear connectors. Engineering Structures, 32(8), 1976-1985.

Casafont, M., Bonada, J., Pastor, M. M., Roure, F., & Susín, A. (2018). Linear buckling analysis of perforated cold-formed steel storage rack columns by means of the generalised beam theory. International Journal of Structural Stability and Dynamics, 18(01), 1850004.

Chapman, J. C., & Balakrishnan, S. (1964). Experiments on composite beams. The Structural Engineer, 42(11), 369-383.

Chromiak, P., & Studnicka, J. (2006). Computer Model for Perfobond Connector. In Proceedings of the International Colloquium on Stability and Ductility of Steel Structures–SDSS.

Chung, K. F., Ho, H. C., Wang, A. J., & Yu, W. K. (2008). Advances in analysis and design of cold-formed steel structures. Advances in Structural Engineering, 11(6), 615-632.

Ciutina, A. L., & stratan, A. (2011). Cyclic performances of shear connectors. In Composite Construction in Steel and Concrete VI (pp. 52-64).

Classen, M., & Hegger, J. (2018). Shear tests on composite dowel rib connectors in cracked concrete. ACI Structural Journal, 115(3), 661-671.

Classen, M., Herbrand, M., Adam, V., Kueres, D., & Sarac, M. (2018). Puzzle-shaped rib shear connectors subjected to combined shear and tension. Journal of Constructional Steel Research, 145, 232-243.

Crisinel, M. (1990). Partial-interaction analysis of composite beams with profiled sheeting and non-welded shear connectors. Journal of Constructional Steel Research, 15(1-2), 65-98.

Dai, X., Lam, D., Sheehan, T., Yang, J., & Zhou, K. (2018, June). Use of bolted shear connectors in composite construction. In Proceedings of the 12th International Conference on Advances in Steel-Concrete Composite Structures. ASCCS 2018 (pp. 475-482). Editorial Universitat Politècnica de València.

Dar, M. A., Subramanian, N., Anbarasu, M., Dar, A. R., & Lim, J. B. (2018). Structural performance of cold-formed steel composite beams. Steel & Composite Structures, 27(5), 545-554.

Dar, M. A., Subramanian, N., Dar, A. R., Anbarasu, M., Lim, J. B., & Atif, M. (2019). Behaviour of partly stiffened cold-formed steel built-up beams: Experimental investigation and numerical validation. Advances in Structural Engineering, 22(1), 172-186.

de Lima Araújo, D., Sales, M. W. R., de Paulo, S. M., & de Cresce El, A. L. H. (2016). Headed steel stud connectors for composite steel beams with precast hollow-core slabs with structural topping. Engineering Structures, 107, 135-150.

Deng, W., Gu, J., Liu, D., Hu, J., & Zhang, J. (2018). Study of single perfobond rib with head stud shear connectors for a composite structure. Magazine of Concrete Research, 71(17), 920-934.

Dhonde, H., Undre, A., Choudekar, G., & Dashputre, T. (2016, May). Fresh and Hardened Properties of Self-Compacting Bacterial Concrete. In Proceedings of the 8th International RILEM Symposium on Self-Compacting Concrete (pp. 287-297).

Ding, F. X., Yin, G. A., Wang, H. B., Wang, L., & Guo, Q. (2017). Static behaviour of stud connectors in bi-direction push-off tests. Thin-Walled Structures, 120, 307-318.

Domone, P. L. (2006). Self-compacting concrete: An analysis of 11 years of case studies. Cement and concrete composites, 28(2), 197-208.

Dubina, D. (2008). Behaviour and performance of cold-formed steel-framed houses under seismic action. Journal of Constructional Steel Research, 64(7-8), 896-913.

Dubina, D., & Ungureanu, V. (2002). Effect of imperfections on numerical simulation of instability behaviour of cold-formed steel members. Thin-walled structures, 40(3), 239-262.

Dubina, D., Ungureanu, V., & Gîlia, L. (2015). Experimental investigations of cold-formed steel beams of corrugated web and built-up section for flanges. Thin-Walled Structures, 90, 159-170.

Dujmovic, D., Androic, B., & Lukacevic, I. (2015). Composite Structures According to Eurocode 4: Worked Examples. John Wiley & Sons.

EFNARC. (2005). The European Guidelines for Self-Compacting Concrete. The European Guidelines for Self-Compacting Concrete, (May), 63. Retrieved from http://www.efnarc.org/pdf/SCCGuidelinesMay2005.pdf

Elinwa, A. U., Ejeh, S. P., & Mamuda, A. M. (2008). Assessing of the fresh concrete properties of self-compacting concrete containing sawdust ash. Construction and building materials, 22(6), 1178-1182.

El-Kassas, E. M. A., Mackie, R. I., & El-Sheikh, A. I. (2002). Using neural networks to predict the design load of cold-formed steel compression members. Advances in Engineering Software, 33(7-10), 713-719.

Ellobody, E., & Young, B. (2005). Structural performance of cold-formed high strength stainless steel columns. Journal of Constructional Steel Research, 61(12), 1631-1649.

Felekoğlu, B., Türkel, S., & Baradan, B. (2007). Effect of water/cement ratio on the fresh and hardened properties of self-compacting concrete. Building and Environment, 42(4), 1795-1802.

Ferreira, L. T. S., de Andrade, S. A. L., & Vellasco, P. D. S. (1998). A design model for bolted composite semi-rigid connections. In Stability and Ductility of Steel Structures (SDSS'97) (pp. 293-306). Pergamon.

Fratamico, D. C., Torabian, S., Zhao, X., Rasmussen, K. J., & Schafer, B. W. (2018). Experiments on the global buckling and collapse of built-up cold-formed steel columns. Journal of Constructional Steel Research, 144, 65-80.

Friberg, B. F. (1954). Frictional resistance under concrete pavements and restraint stresses in long reinforced slabs. In Highway Research Board Proceedings (Vol. 33).

Galjaard, H. J., & Walraven, J. C. (2001). Behaviour of different types of shear connectors for steel-concrete structures. In Structural Engineering, Mechanics and Computation (pp. 385-392). Elsevier Science.

Gambhir, M. L. (2013). Concrete technology: theory and practice. Tata McGraw-Hill Education.

García, A. R., & Arrizabalaga, E. M. (2004). Design of composite beams using light steel sections (Doctoral dissertation, Universitat Politècnica de Catalunya. Escola Tècnica Superior d'Enginyers de Camins, Canals i Ports de Barcelona. Departament d'Enginyeria de la Construcció, 2004 (Enginyeria de Camins, Canals i Ports)).

Gardner, L., Bu, Y., & Theofanous, M. (2016). Laser-welded stainless steel I-sections: Residual stress measurements and column buckling tests. Engineering Structures, 127, 536-548.

Gelfi, P., Giuriani, E., & Marini, A. (2002). Stud shear connection design for composite concrete slab and wood beams. Journal of Structural Engineering, 128(12), 1544-1550.

Ghersi, A., Mazzolani, F., & Landolfo, R. (2014). Design of metallic cold-formed thin-walled members. CRC Press.

Goodier, C. I. (2003). Development of self-compacting concrete.

Gu, J. C., Liu, D., Deng, W. Q., & Zhang, J. D. (2019). Experimental study on the shear resistance of a comb-type perfobond rib shear connector. Journal of Constructional Steel Research, 158, 279-289.

Güneyisi, E. (2010). Fresh properties of self-compacting rubberized concrete incorporated with fly ash. Materials and structures, 43(8), 1037-1048.

Guzelbey, I. H., Cevik, A., & Erklig, A. (2006). Prediction of web crippling strength of cold-formed steel sheetings using neural networks. Journal of Constructional Steel Research, 62(10), 962-973.

Hällmark, R., Collin, P., & Hicks, S. J. (2019). Post-installed shear connectors: Push-out tests of coiled spring pins vs. headed studs. Journal of Constructional Steel Research, 161, 1-16.

Han, Q., Wang, Y., Xu, J., Xing, Y., & Yang, G. (2017). Numerical analysis on shear stud in push-out test with crumb rubber concrete. Journal of Constructional Steel Research, 130, 148-158.

Hanaor, A. (2000). Tests of composite beams with cold-formed sections. Journal of Constructional Steel Research, 54(2), 245-264.

Hancock, G. J. (1998). Design of Cold-formed Steel Structures: To Australian/New Zealand Standard AS/NZS 4600: 1996. Australian Institute of Steel Construction.

Hancock, G. J. (2003). Cold-formed steel structures. Journal of constructional steel research, 59(4), 473-487.

He, S., Fang, Z., & Mosallam, A. S. (2017). Push-out tests for perfobond strip connectors with UHPC grout in the joints of steel-concrete hybrid bridge girders. Engineering Structures, 135, 177-190.

He, S., Fang, Z., Fang, Y., Liu, M., Liu, L., & Mosallam, A. S. (2016). Experimental study on perfobond strip connector in steel–concrete joints of hybrid bridges. Journal of Constructional Steel Research, 118, 169-179.

Hegger, J., Sedlacek, G., Döinghaus, P., Trumpf, H., & Eligehausen, R. (2001, September). Studies on the ductility of shear connectors when using high-strength steel and high-strength concrete. In International symposium on connections between steel and concrete (pp. 1025-1045). RILEM Publications SARL.

Hegyi, P., & Dunai, L. (2016). Experimental study on ultra-lightweight-concrete encased cold-formed steel structures Part I: Stability behaviour of elements subjected to bending. Thin-Walled Structures, 101, 75-84.

Higgins, A. (2005). Design of All-bolted Extended Double Angle, Single Angle, and Tee Shear Connections (Doctoral dissertation, University of Florida).

Holesapple, M. W., & LaBoube, R. A. (2003). Web crippling of cold-formed steel beams at end supports. Engineering structures, 25(9), 1211-1216.

Hsu, C. T. T., Punurai, S., Punurai, W., & Majdi, Y. (2014). New composite beams having cold-formed steel joists and concrete slab. Engineering structures, 71, 187-200.

Hui, C. (2014). Moment redistribution in cold-formed steel purlin systems (Doctoral dissertation, Imperial College London).

Huo, J., Wang, H., Li, L., & Liu, Y. (2019). Experimental study on impact behaviour of stud shear connectors in composite beams with profiled steel sheeting. Journal of Constructional Steel Research, 161, 436-449.

Irwan, J. M., Hanizah, A. H., & Azmi, I. (2009). Test of shear transfer enhancement in symmetric cold-formed steel–concrete composite beams. Journal of Constructional Steel Research, 65(12), 2087-2098.

Irwan, J. M., Hanizah, A. H., Azmi, I., & Koh, H. B. (2011). Large-scale test of symmetric cold-formed steel (CFS)–concrete composite beams with BTTST enhancement. Journal of Constructional Steel Research, 67(4), 720-726.

Jiang, L., Liu, Y., & Fam, A. (2019). Stress concentration factors in concrete-filled square hollow section joints with perfobond ribs. Engineering Structures, 181, 165-180.

Johnson, R. P. (2005). Shear connection in beams that support composite slabs-BS 5950 and EN 1994-1-1. Structural Engineer, 83(22), 21-24.

Johnson, R. P., & Anderson, D. (2004). Designers' Guide to EN 1994-1-1: Eurocode 4: Design of Composite Steel and Concrete Structures. General Rules and Rules for Buildings. Thomas Telford.

Kapoor, Y. P. (2003). Self-Compacting Concrete an Economical Approach.

Karabulut, B., & Soyoz, S. (2017). Experimental and analytical studies on different configurations of cold-formed steel structures. Journal of Constructional Steel Research, 133, 535-546.

Kim, J. S., Kwark, J., Joh, C., Yoo, S. W., & Lee, K. C. (2015). Headed stud shear connector for thin ultrahigh-performance concrete bridge deck. Journal of Constructional Steel Research, 108, 23-30.

Kim, K. S., Han, O., Choi, J., & Kim, S. H. (2019). Hysteretic performance of stubby Y-type perfobond rib shear connectors depending on transverse rebar. Construction and Building Materials, 200, 64-79.

Kim, S. H., Choi, J., Park, S. J., Ahn, J. H., & Jung, C. Y. (2014). Behaviour of composite girder with Y-type perfobond rib shear connectors. Journal of Constructional Steel Research, 103, 275-289.

Kim, S. H., Choi, K. T., Park, S. J., Park, S. M., & Jung, C. Y. (2013). Experimental shear resistance evaluation of Y-type perfobond rib shear connector. Journal of constructional steel research, 82, 1-18.

Kim, S. H., Kim, K. S., Han, O., & Park, J. S. (2018). Influence of transverse rebar on shear behaviour of Y-type perfobond rib shear connection. Construction and Building Materials, 180, 254-264.

Kim, S. H., Park, S. J., Heo, W. H., & Jung, C. Y. (2015). Shear resistance characteristic and ductility of Y-type perfobond rib shear connector. Steel and Composite Structures, 18(2), 497-517.

Kolarkar, P., & Mahendran, M. (2012). Experimental studies of non-load bearing steel wall systems under fire conditions. Fire safety journal, 53, 85-104.

Kruszewski, D., Wille, K., & Zaghi, A. E. (2018). Push-out behaviour of headed shear studs welded on thin plates and embedded in UHPC. Engineering Structures, 173, 429-441.

Kumar, M. A., & Kalyanaraman, V. (2012). Design strength of locally buckling stub-lipped channel columns. Journal of Structural Engineering, 138(11), 1291-1299.

Kwon, G., Engelhardt, M. D., & Klingner, R. E. (2010). Behaviour of post-installed shear connectors under static and fatigue loading. Journal of Constructional Steel Research, 66(4), 532-541.

Kyvelou, P., Gardner, L., & Nethercot, D. A. (2017). Testing and Analysis of Composite Cold-Formed Steel and Wood− Based Flooring Systems. Journal of Structural Engineering, 143(11), 04017146.

Kyvelou, P., Gardner, L., & Nethercot, D. A. (2018). Finite element modelling of composite cold-formed steel flooring systems. Engineering Structures, 158, 28-42.

LaBoube, R. A., & Findlay, P. F. (2007). Wall stud-to-track gap: Experimental investigation. Journal of architectural engineering, 13(2), 105-110.

Lakkavalli, B. S., & Liu, Y. (2006). Experimental study of composite cold-formed steel C-section floor joists. Journal of Constructional Steel Research, 62(10), 995-1006.

Lam, D., & El-Lobody, E. (2005). Behaviour of headed stud shear connectors in composite beam. Journal of Structural Engineering, 131(1), 96-107.

Lam, D., Dai, X., Ashour, A., & Rehman, N. (2017). Recent research on composite beams with demountable shear connectors. Steel Construction, 10(2), 125-134.

Lam, D., Elliott, K. S., & Nethercot, D. A. (2000). Parametric study on composite steel beams with precast concrete hollow core floor slabs. Journal of Constructional Steel Research, 54(2), 283-304.

Lau, S. C., & Hancock, G. J. (1987). Distortional buckling formulas for channel columns. Journal of Structural Engineering, 113(5), 1063-1078.

Lawan, M. M. (2015). Structural Pereormance of Cold-formed Steel with Self-compacting Concrete in a Composite Beam System (Doctoral dissertation, Universiti Teknologi Malaysia).

Lawan, M. M., Shek, P. N., & Tahir, M. M. (2018). Comparative Study between Linear-Interpolation and Stress-Block Methods of Composite Design Using Cold-Formed Steel Section. International Journal of Engineering & Technology, 7(3.9), 38-41.

Lawan, M. M., Tahir, M. M., & Hosseinpour, E. (2016). Feasibility of Using Bolted Shear Connector with Cold-Formed Steel in Composite Construction. Jurnal Teknologi, 78(6-12).

Lawan, M. M., Tahir, M. M., & Mirza, J. (2016). Bolted Shear connectors performance in self-compacting concrete integrated with cold-formed steel section. Latin American Journal of Solids and Structures, 13(4), 731-749.

Lawan, M. M., Tahir, M. M., Ngian, S. P., & Sulaiman, A. (2015). Structural Performance of Cold-Formed Steel Section in Composite Structures: A Review. Jurnal Teknologi, 74(4).

Łaźniewska-Piekarczyk, B. (2013). The type of air-entraining and viscosity modifying admixtures and porosity and frost durability of high performance self-compacting concrete. Construction and Building Materials, 40, 659-671.

Lee, P. G., Shim, C. S., & Chang, S. P. (2005). Static and fatigue behaviour of large stud shear connectors for steel–concrete composite bridges. Journal of constructional steel research, 61(9), 1270-1285.

Lee, Y. H., Tan, C. S., Mohammad, S., Md Tahir, M., & Shek, P. N. (2014). Review on cold-formed steel connections. The Scientific World Journal, 2014.

Leemann, A., & Hoffmann, C. (2005). Properties of self-compacting and conventional concrete–differences and similarities. Magazine of Concrete Research, 57(6), 315-319.

Leonhardt, E. F., Andra, W., Andra, H. P., & Harre, W. (1987). New improved shear connector with high fatigue strength for composite structures. Neues vorteilhaftes Verbundmittel fur stahlverbund-Tragwerke mit hoher Danerfestigkeit), Beton-Und Stahlbetoubau, 12, 325-331.

Li, N., Long, G., Ma, C., Fu, Q., Zeng, X., Ma, K., ... & Luo, B. (2019). Properties of self-compacting concrete (SCC) with recycled tire rubber aggregate: a comprehensive study. Journal of Cleaner Production, 236, 117707.

Li, Y. L., Li, Y. Q., & Shen, Z. Y. (2016). Investigation on flexural strength of cold-formed thin-walled steel beams with built-up box section. Thin-Walled Structures, 107, 66-79.

Li, Z., & Schafer, B. W. (2010). Buckling analysis of cold-formed steel members with general boundary conditions using CUFSM conventional and constrained finite strip methods.

Lim, J. B., & Nethercot, D. A. (2004). Stiffness prediction for bolted moment-connections between cold-formed steel members. Journal of constructional steel research, 60(1), 85-107.

Lim, J. S., Kim, T. S., & Kim, S. H. (2013). Ultimate strength of single shear bolted connections with cold-formed ferritic stainless steel. Journal of Zhejiang University SCIENCE A, 14(2), 120-136.

Liu, J., Zhao, Y., Yang, Y., & Chen, Y. F. (2019). Bending Capacity and Elastic Stiffness for a Novel Configuration of Cold-Formed U-Shaped Steel-and-Concrete Composite Beams. Journal of Structural Engineering, 145(10), 04019106.

Liu, X., Bradford, M. A., Chen, Q. J., & Ban, H. (2016). Finite element modelling of steel–concrete composite beams with high-strength friction-grip bolt shear connectors. Finite Elements in Analysis and Design, 108, 54-65.

Liu, Y., Guo, L., Qu, B., & Zhang, S. (2017). Experimental investigation on the flexural behaviour of steel-concrete composite beams with U-shaped steel girders and angle connectors. Engineering Structures, 131, 492-502.

Loucks, J. F., & Harry, G. (1926). U.S. Patent No. 1,574,586. Washington, DC: U.S. Patent and Trademark Office.

Macdonald, M., & Heiyantuduwa, M. A. (2012). A design rule for web crippling of cold-formed steel lipped channel beams based on nonlinear FEA. Thin-Walled Structures, 53, 123-130.

Macdonald, M., Don, M. H., Kotełko, M., & Rhodes, J. (2011). Web crippling behaviour of thin-walled lipped channel beams. Thin-Walled Structures, 49(5), 682-690.

Madandoust, R., & Mousavi, S. Y. (2012). Fresh and hardened properties of self-compacting concrete containing metakaolin. Construction and Building Materials, 35, 752-760.

Maleki, S., & Bagheri, S. (2008). Behaviour of channel shear connectors, Part I: Experimental study. Journal of Constructional Steel Research, 64(12), 1333-1340.

Maleki, S., & Bagheri, S. (2008). Behaviour of channel shear connectors, Part II: Analytical study. Journal of Constructional Steel Research, 64(12), 1341-1348.

Marcello Tarantino, A., & Dezi, L. (1992). Creep effects in composite beams with flexible shear connectors. Journal of Structural Engineering, 118(8), 2063-2080.

Marshall, W. T., Nelson, H. M., & Banerjee, H. K. (1971). An Experiment Study of the Use of High-Strength Friction Grip Bolts as Shear Connectors in Composite Beams. Structural Engineer.

Matus, R. A., & Jullien, J. F. (1996, June). A new shear stud connector proposal. In Composite Construction in Steel and Concrete III (pp. 298-311). ASCE.

Mirza, O., & Uy, B. (2010). Effects of the combination of axial and shear loading on the behaviour of headed stud steel anchors. Engineering Structures, 32(1), 93-105.

Moy, S. S. J., & Tayler, C. (1996). The effect of precast concrete planks on shear connector strength. Journal of Constructional Steel Research, 36(3), 201-213.

Moynihan, M. C., & Allwood, J. M. (2014). Viability and performance of demountable composite connectors. Journal of Constructional Steel Research, 99, 47-56.

Nakajima, A., Koseki, S., Hashimoto, M., Suzuki, Y., & Nguyen, M. H. (2012). Evaluation of shear resistance of perfobond strip based on simple push-out test. Journal of Japan Society of Civil Engineers, Ser. A1 (Structural Engineering & Earthquake Engineering (SE/EE)), 68, 495-508.

Nguyen, H. T., & Kim, S. E. (2009). Finite element modeling of push-out tests for large stud shear connectors. Journal of Constructional Steel Research, 65(10-11), 1909-1920.

Nguyen, R. P. (1991). Thin-walled, cold-formed steel composite beams. Journal of Structural Engineering, 117(10), 2936-2952.

Nili, M., Sasanipour, H., & Aslani, F. (2019). The Effect of Fine and Coarse Recycled Aggregates on Fresh and Mechanical Properties of Self-Compacting Concrete. Materials, 12(7), 1120.

Nuruddin, M. F., Chang, K. Y., & Azmee, N. M. (2014). Workability and compressive strength of ductile self-compacting concrete (DSCC) with various cement replacement materials. Construction and Building Materials, 55, 153-157.

Oguejiofor, E. C., & Hosain, M. U. (1992). Behaviour of perfobond rib shear connectors in composite beams: full-size tests. Canadian Journal of Civil Engineering, 19(2), 224-235.

Oguejiofor, E. C., & Hosain, M. U. (1992). Perfobond rib connectors for composite beams. In Composite Construction in Steel and Concrete II (pp. 883-898). ASCE.

Oguejiofor, E. C., & Hosain, M. U. (1994). A parametric study of perfobond rib shear connectors. Canadian Journal of Civil Engineering, 21(4), 614-625.

Okamura, H., Ozawa, K., & Ouchi, M. (2000). Self-compacting concrete. structural Concrete, 1(1), 3-17.

Ouchi, M., Nakamura, S. A., Osterberg, T., Hallberg, S., & Lwin, M. (2003). Applications of self-compacting concrete in Japan, Europe and the United States. Kochi University of Technology, Kochi, Japan.

Pala, M. (2008). Genetic programming-based formulation for distortional buckling stress of cold-formed steel members. Journal of Constructional Steel Research, 64(12), 1495-1504.

Park, S. (1992). EN 1994-Eurocode 4: Design of composite steel and concrete structures.

Parra, C., Valcuende, M., & Gómez, F. (2011). Splitting tensile strength and modulus of elasticity of self-compacting concrete. Construction and Building materials, 25(1), 201-207.

Pashan, A. (2006). Behaviour of channel shear connectors: push-out tests (Doctoral dissertation, University of Saskatchewan).

Pavlović, M., Marković, Z., Veljković, M., & Buđevac, D. (2013). Bolted shear connectors vs. headed studs' behaviour in push-out tests. Journal of Constructional Steel Research, 88, 134-149.

Persson, B. (2001). A comparison between mechanical properties of self-compacting concrete and the corresponding properties of normal concrete. Cement and concrete Research, 31(2), 193-198.

Porter, M. L., Ekberg Jr, C. E., Greimann, L. F., & Elleby, H. A. (1976). Shear-bond analysis of steel-deck-reinforced slabs. Journal of the structural Division, 102(Proc. Paper 12625).

Qi, J., Hu, Y., Wang, J., & Li, W. (2019). Behaviour and strength of headed stud shear connectors in ultra-high-performance concrete of composite bridges. Frontiers of Structural and Civil Engineering, 13(5), 1138-1149.

Qureshi, J., Lam, D., & Ye, J. (2009). Behaviour of headed shear stud in a push test using profiled steel sheeting. In Proceedings of the 9th international conference on steel concrete composite and hybrid structures.

Ranawaka, T., & Mahendran, M. (2009). Experimental study of the mechanical properties of light gauge cold-formed steels at elevated temperatures. Fire Safety Journal, 44(2), 219-229.

Rao, S. N. (1970). Composite Construction-Tests on Small Scale Shear Connectors. The Institute of Engineers, Australia. Civil Engineering Transactions, April.

Ren, Q., Jiang, Z., Li, H., Zhu, X., & Chen, Q. (2019). Fresh and hardened properties of self-compacting concrete using silicon carbide waste as a viscosity-modifying agent. Construction and Building Materials, 200, 324-332.

Reyes, W., & Guzmán, A. (2011). Evaluation of the slenderness ratio in built-up cold-formed box sections. Journal of Constructional Steel Research, 67(6), 929-935.

Rogers, C. A., & Hancock, G. J. (1997). Ductility of G550 sheet steels in tension. Journal of Structural Engineering, 123(12), 1586-1594.

Roik, K., & Lungershausen, H. (1989). Shear resistance of headed stud shear connectors in concrete slabs with profiled steel sheeting. Stahlbau, 58(9), 269-273.

Saggaff, A., Alhajri, T., Alenezi, K., Tahir, M. M., Zin, R. M., Ngian, S. P., & Ragaee, M. (2016). Experimental Study on Bolted Shear Connector Enhancement in Precast Cold-Formed Steel-Ferro Cement For Composite Beam System. Iioab Journal, 7, 446-452.

Saggaff, A., Lawan, M. M., Tahir, M. M., & Mirza, J. (2015). Impact of Shear Connector Spacing in Composite Construction Incorporating Cold-Formed Steel Channel Lipped Section. Abstract of Emerging Trends in Scientific Research, 4, 1-13.

Salih, M. N., Tahir, M. M., Mohammad, S., & Ahmad, Y. (2018, November). Behaviour of Boxed Cold-Formed Steel as Composite Beam with Rebar as Shear Connector. In International Congress and Exhibition" Sustainable Civil Infrastructures: Innovative Infrastructure Geotechnology" (pp. 324-332). Springer, Cham.

Salih, M. N., Tahir, M. M., Mohammad, S., Ahmad, Y., Sulaiman, A., Shek, P. N., ... & Aminuddin, K. M. (2019, April). Experimental study on flexural behaviour of partially encased cold-formed steel composite beams using rebar as shear connector. In IOP Conference Series: Materials Science and Engineering (Vol. 513, No. 1, p. 012038). IOP Publishing.

Schafer, B. W. (2002). Local, distortional, and Euler buckling of thin-walled columns. Journal of structural engineering, 128(3), 289-299.

Schuster, R. M. (1970). Strength and behaviour of cold-rolled steel-deck-reinforced concrete floor slabs.

Sedghi, Y., Zandi, Y., Toghroli, A., Safa, M., Mohamad, E. T., Khorami, M., & Wakil, K. (2018). Application of ANFIS technique on performance of C and L shaped angle shear connectors. Smart Struct Syst, 22(3), 335-340.

Selby, D. A. (1993). U.S. Patent No. 5,220,761. Washington, DC: U.S. Patent and Trademark Office.

Shan, M. Y., LaBoube, R. A., & Yu, W. W. (1993). Shear behaviour of web elements with openings. In Proc. Annual Technical Session of the Structural Stability Research Council. Structural Stability Research Council Milwaukee, WI.

Shariati, A., Sulong, N. R., Suhatril, M., & Shariati, M. (2012). Investigation of channel shear connectors for composite concrete and steel T-beam. International journal of physical sciences, 7(11), 1828-1831.

Shariati, M., Rafiei, S., Zandi, Y., Fooladvand, R., Gharehaghaj, B., Shariat, A., ... & Poi-Ngian, S. (2019). Experimental investigation on the effect of cementitious materials on fresh and mechanical properties of self-consolidating concrete. Advances in concrete construction, 8(3), 225-237.

Shariati, M., Sulong, N. R., KH, M. A., & Mahoutian, M. (2011). Shear resistance of channel shear connectors in plain, reinforced and lightweight concrete. Scientific research and essays, 6(4), 977-983.

Shim, C. S., Kim, D. W., & Nhat, M. X. (2014). Performance of stud clusters in precast bridge decks The Baltic Journal of Road and Bridge Engineering, 9(1), 43-43.

Shim, C. S., Lee, P. G., & Yoon, T. Y. (2004). Static behaviour of large stud shear connectors. Engineering structures, 26(12), 1853-1860.

Shim, C. S., Lee, P. G., Kim, D. W., & Chung, C. H. (2011). Effects of group arrangement on the ultimate strength of stud shear connection. In Composite Construction in Steel and Concrete VI (pp. 92-101).

Sivakumaran, K. S. (1987). Natural frequencies of symmetrically laminated rectangular plates with free edges. Composite structures, 7(3), 191-204.

Smith, S. T., Bradford, M. A., & Oehlers, D. J. (1999). Elastic buckling of unilaterally constrained rectangular plates in pure shear. Engineering Structures, 21(5), 443-453.

Standard, I. (2006). ISO 15614-6: Specification and qualification of welding procedures for metallic materials — Welding procedure test part 6. Order A Journal on The Theory Of Ordered Sets And Its Applications, 2006.

Stark, J. B. (1989). Composite steel and concrete beams with partial shear connection. Heron (Delft), 34(4), 1-63.

Stephens, S. F., & LaBoube, R. A. (2003). Web crippling and combined bending and web crippling of cold-formed steel beam headers. Thin-walled structures, 41(12), 1073-1087.

Tani, S., & Fujii, K. (2019). ULTIMATE STRIP STRENGTH OF PERFOBOND STRIP WITH SMALL HOLE CONFINED BY CONCRETE COVER. International Journal, 17(63), 233-240.

Timoshenko, S., & Gere, J. M. (1961). Theory of elasticity stability. McGraw.

Toghroli, A., Mohammadhassani, M., Suhatril, M., Shariati, M., & Ibrahim, Z. (2014). Prediction of shear capacity of channel shear connectors using the ANFIS model. Steel Compos Struct, 17(5), 623-639.

Ungureanu, V., Kotełko, M., Karmazyn, A., & Dubina, D. (2018). Plastic mechanisms of thin-walled cold-formed steel members in eccentric compression. Thin-Walled Structures, 128, 184-192.

Valente, I., & Cruz, P. J. (2004). Experimental studies on shear connection between steel and lightweight concrete.

Veldanda, M. R., & Hosain, M. U. (1992). Behaviour of perfobond rib shear connectors: push-out tests. Canadian Journal of Civil Engineering, 19(1), 1-10.

Veríssimo, G. S., Paes, J. R., Valente, I., Cruz, P. J., & Fakury, R. H. (2006). Design and experimental analysis of a new shear connector for steel and concrete composite structures. In Proceedings of the 3rd International Conference on Bridge Maintenance, Safety and Management-Bridge Maintenance, Safety, Management, Life-Cycle Performance and Cost (pp. 807-809). Taylor & Francis.

Vianna, J. D. C., Costa-Neves, L. F., Vellasco, P. D. S., & de Andrade, S. A. L. (2008). Structural behaviour of T-Perfobond shear connectors in composite girders: An experimental approach. Engineering Structures, 30(9), 2381-2391.

Vianna, J. D. C., Costa-Neves, L. F., Vellasco, P. D. S., & De Andrade, S. A. L. (2009). Experimental assessment of Perfobond and T-Perfobond shear connectors' structural response. Journal of Constructional Steel Research, 65(2), 408-421.

Viest, I. M. (1951). Full-scale tests of channel shear connectors and composite t-beams. University of Illinois at Urbana Champaign, College of Engineering. Engineering Experiment Station.

Viest, I. M., Colaco, J. P., Furlong, R. W., Griffis, L. G., Leon, R. T., & Wyllie, L. A. (1997). Composite construction design for buildings (pp. 4-1). New York: McGraw-Hill.

Wang, J., Xu, Q., Yao, Y., Qi, J., & Xiu, H. (2018). Static behaviour of grouped large headed stud-UHPC shear connectors in composite structures. Composite Structures, 206, 202-214.

Wang, L., & Young, B. (2015). Behaviour of cold-formed steel built-up sections with intermediate stiffeners under bending. I: Tests and numerical validation. Journal of Structural Engineering, 142(3), 04015150.

Wang, Y. C. (1998). Deflection of steel-concrete composite beams with partial shear interaction. Journal of Structural Engineering, 124(10), 1159-1165.

Wang, Z., Zhao, C., & LI, Q. (2011). Experimental investigation on load-slip relationship of perfobond rib shear connectors. Journal of Southwest Jiaotong University, 46(4), 547-552.

Wehbe, N., Bahmani, P., & Wehbe, A. (2013). Behaviour of concrete/cold formed steel composite beams: Experimental development of a novel structural system. International Journal of Concrete Structures and Materials, 7(1), 51-59.

Wilkinson, T., & Hancock, G. (2002). Predicting the rotation capacity of cold-formed RHS beams using finite element analysis. Journal of Constructional Steel Research, 58(11), 1455-1471.

Xie, J., Zhu, G. R., & Yan, J. B. (2018). Mechanical properties of headed studs at low temperatures in Arctic infrastructure. Journal of Constructional Steel Research, 149, 130-140.

Xu, L., Sultana, P., & Zhou, X. (2009). Flexural strength of cold-formed steel built-up box sections. Thin-Walled Structures, 47(6-7), 807-815.

Xue, W., Ding, M., Wang, H., & Luo, Z. (2008). Static behaviour and theoretical model of stud shear connectors. Journal of bridge engineering, 13(6), 623-634.

Yamaki, N. (1959). Postbuckling behaviour of rectangular plates with small initial curvature loaded in edge compression. Trans. ASME, J. Appl. Mech., 26, 407-414.

Yan, J. B., & Xie, J. (2018). Shear Behaviour of Headed Stud Connectors at Low Temperatures Relevant to the Arctic Environment. Journal of Structural Engineering, 144(9), 04018139.

Ye, J., Hajirasouliha, I., Becque, J., & Pilakoutas, K. (2016). Development of more efficient cold-formed steel channel sections in bending. Thin-walled structures, 101, 1-13.

Young, B. (2004). Tests and design of fixed-ended cold-formed steel plain angle columns. Journal of structural engineering, 130(12), 1931-1940.

Young, B., & Ellobody, E. (2005, January). Finite element analysis of cold-formed Steel lipped angle compression members. In Fourth International Conference on Advances in Steel Structures (pp. 469-478). Elsevier Science Ltd.

Yu, C., & Schafer, B. W. (2003). Local buckling tests on cold-formed steel beams. Journal of Structural Engineering, 129(12), 1596-1606.

Yu, C., & Schafer, B. W. (2006). Distortional buckling tests on cold-formed steel beams. Journal of structural engineering, 132(4), 515-528.

Yu, W. W., & LaBoube, R. A. (2019). Cold-formed steel design. John Wiley & Sons.

Zellner, W. (1988). Recent designs of composite bridges and a new type of shear connectors. Composite Construction in Steel and Concrete.

Zhao, C., Li, Z., Deng, K., & Wang, W. (2018). Experimental investigation on the bearing mechanism of Perfobond rib shear connectors. Engineering Structures, 159, 172-184.

Zheng, S., Liu, Y., Liu, Y., & Zhao, C. (2019). Experimental and numerical study on shear resistance of notched perfobond shear connector. Materials, 12(3), 341.

Zheng, S., Zhao, C., & Liu, Y. (2019). Analytical model for load–slip relationship of perfobond shear connector based on push-out test. Materials, 12(1), 29.

Zhou, X., Zhao, Y., Liu, J., Chen, Y. F., & Yang, Y. (2019). Bending experiment on a novel configuration of cold-formed U-shaped steel-concrete composite beams. Engineering Structures, 180, 124-133.

Zhu, W., Gibbs, J. C., & Bartos, P. J. (2001). Uniformity of in situ properties of self-compacting concrete in full-scale structural elements. Cement and concrete composites, 23(1), 57-64.

Zingoni, A. (2001, March). Behaviour of Different Types of Shear Connectors for Steel-Concrete Structures. In Structural Engineering, Mechanics, and Computation: Proceedings of the International Conference on Structural

Engineering, Mechanics, and Computation, 2-4 April 2001, Cape Town, South Africa (Vol. 1, p. 385). Elsevier.

APPENDIX A

Self-Compacting Concrete Detailed Mix Design

	Design Calculation	Issue date:			17/01/2018
1.1	Characteristic Strength (BS 8110-1 & BS 5328-1)	(Specified)	=	40,0 N/mm^2	
1.2	Proportion of results below characteristic strength		=	5%	
1.3	Margin		=	7,5 N/mm^2	
1.4	Free Water / Cement Ratio	(A)	=	0,44	
2.1	Admixture Type (dosage Rate Per 1 m^3) Superplasticiser		=	4,69 Liter	(AF333)
	Water Reducer		=	1,03 Liter	(WR96M)
2.2	Specific gravity of cement		=	3,00	
2.3	Specific gravity of combined	(D)	=	2,61 (SS)	
3.1	Maximum aggregate size	(Specified)	=	10,0 mm	
3.2	Grading of fine aggregate				
3.3	Proportion of fine	(B)	=	60%	
3.4	Proportion of course	(C)	=	40%	
4.1	Workability: slump	(Specified)	=	600 +/- 50	
4.2	Air Content (estimated)	(E)	=	8%	
4.3	Free water requirement	(F)	=	206 kg/m^3	
4.4	Cementitious content	(G)	=	470 kg/m^3	
4.5	Total aggregate content	(H)	=	1628 kg/m^3	
4.6	Total concrete volume				
4.7	Fine aggregate (H x B %)	(J)	=	978 kg/m^3	
4.8	Coarse Aggregate (H x C%)	(K)	=	650 kg/m^3	
5.1	Designed Density of Concrete (F + G + J + K)		=	2304 kg/m^3	

SUMMARY

Grade	=	40 N/mm^2	
Specified	=	600 +/- 50	
Batch Weights (SSD) for one cubic metre of concrete			
Cementitious (Mascrete Eco)	=	470 kg/m^3	
Fine Aggregate - Sand	=	978 kg/m^3	
Coarse Aggregate (10 mm)	=	650 kg/m^3	
Admixture			
Superplasticiser	=	4,69 Liter	(AF333)
Water Reducer	=	1,03 Liter	(WR96M)

APPENDIX B

Design Calculations of Cold-Formed Steel Section Design

EFFECTIVE SECTION OF LIPPED-CHANNEL

2. Effective section of lipped channel for bending

2.1. Data of lipped channel

REF : DESIGN OF COLD-FORMED STEEL STRUCTURES
: WILEY BLACKWELL - DAN DUBINA
: EX 3.1-P146

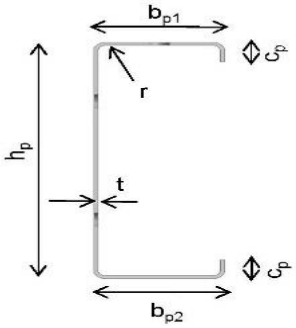

The dimensions of the cross section and the material properties are:

Method	:			=	Constant	
Profil	:			=	25024	
h	:	Total height		=	250	mm
b_1	:	Total width of flange in compression		=	75	mm
b_2	:	Total width of flange in tension		=	75	mm
c	:	Total width of edge fold		=	20	mm
r	:	Internal radius		=	5	mm
t_{nom}	:	Nominal thickness		=	2.4	mm
t_{coat}	:			=	0.04	mm
t	:	Steel core thk	$t_{nom} - t_{coat}$	=	2.36	mm
f_{yb}	:	Basic yield strength		=	524	Mpa
E_s	:	Modulus of elasticity		=	216963	Mpa
v	:	Poisson's ratio		=	0.3	
γ_{M0}	:	Partial factor		=	1	

The dimensions of the section centre line are:

h_p	:	$h - t_{nom}$	=	247.6	mm
b_{p1}	:	$b_1 - t_{nom}$	=	72.6	mm
b_{p2}	:	$b_2 - t_{nom}$	=	72.6	mm
c_p	:	$c - t_{nom} / 2$	=	18.8	mm

2.2. Geometrical proportions geometrical proportions

2.2.1 Checking of geometrical proportions

The design method of EN1993-1-3 can be applied if the following conditions are satisfied:

b / t	≤	60	b_1 / t	-- >	31.78	<	60	OK
c / t	≤	50	c / t	-- >	8.4746	<	50	OK
h / t	≤	500	h / t	-- >	105.93	<	500	OK

In the order to rovide sufficient stiffness and to avoid primary buckling of the stiffener itself, the size of siffener should be within the following range :

0.2	≤	c / b_1	≤	0.6	
0.2	≤	0.267	<	0.6	OK

And

0.2	≤	c / b_2	≤	0.6	
0.2	≤	0.267	<	0.6	OK

The influence of rounding of the corners is neglected if:

r / t	≤	5
2.119	<	5 OK

And

r / b_{p1}	≤	0.1
0.069	<	0.1 OK

And

r / b_{p2}	≤	0.1
0.069	<	0.1 OK

Therefore the geometrical proportional status for channel is OK

2.2.2 Gross section properties

Gross section with mid-line procedures

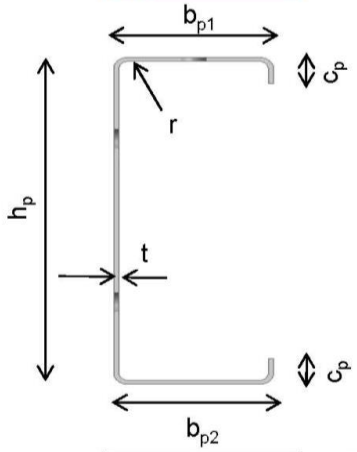

	B mm		T mm	A mm^2
c_p =	18.8	t =	2.36	44.368
b_{p1} =	72.6	t =	2.36	171.34
h_p =	247.6	t =	2.36	584.34
b_{p2} =	72.6	t =	2.36	171.34
c_p =	18.8	t =	2.36	44.368
TOTAL				1015.7

A_{br} : ΣA_i = 1015.744 mm^2

2.2.3 Neutral axis with respect to Z

Position of the neutral axis with respect to the flange in compression:

Statis moment with respect to the flange in compression

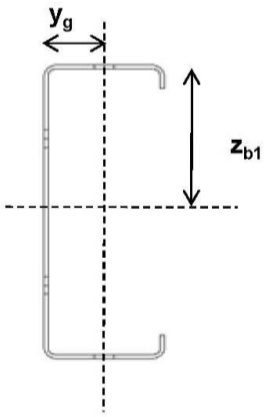

	B mm		T mm		Z mm			A Z mm^3
c_p =	18.8	t =	2.36	$h_p - c_p/2$	=	238.2	10568.4576
b_{p1} =	72.6	t =	2.36	0	=	0	0
h_p =	247.6	t =	2.36	$h_p / 2$	=	123.8	72340.7968
b_{p2} =	72.6	t =	2.36	h_p	=	247.6	42422.7936
c_p =	18.8	t =	2.36	$c_p / 2$	=	9.4	417.0592
TOTAL							125749.1072

Σ A Z : = 125749.1072 mm^3

z_{b1} : Σ A Z / A_{br} = 123.800 mm

2.2.4 Neutral axis with respect to Y

Position of the neutral axis with respect to the web

B mm		T mm		Y mm		A Z mm^3
c_p =	18.8	t =	2.36	b_{p1} =	72.6	3221.1168
b_{p1} =	72.6	t =	2.36	b_{p1} / 2 =	36.3	6219.4968
b_{p2} =	72.6	t =	2.36	b_{p2} / 2 =	36.3	6219.4968
c_p =	18.8	t =	2.36	b_{p2} =	72.6	3221.1168
TOTAL						18881.2272

Σ A Y : = 18881.2272 mm^2

The horizontal position of the neutral axis from the centre line of the web for the gross cross section y_g is :

y_g : Σ A Y / A_{br} = 18.589 mm

2.3. Plane element without stiffner

The effective widths of compression elements shall be obtained from Table below for doubly supported compression elements or for outstand compression elements (CEN, 2006b). The reduction factor ρ used in Tables below to determine beff shall be based on the largest compressive stress σcom,Ed in the relevant element (calculated on the basis of the effective cross section and taking account of possible second order effects), when the resistance of the cross section is reached.

Table 1. Internal compression elements

Table 3.5 – Internal compression elements

Stress distribution (compression positive)	Effective width b_{eff}
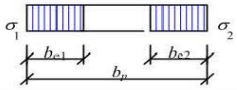	$\psi = 1$ $b_{eff} = \rho \cdot b_p$ $b_{e1} = 0.5 \cdot b_{eff}; b_{e2} = 0.5 \cdot b_{eff}$
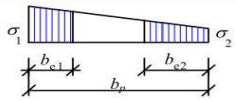	$1 > \psi \geq 0$ $b_{eff} = \rho \cdot b_p$ $b_{e1} = \frac{2}{5-\psi} \cdot b_{eff}; b_{e2} = b_{eff} - b_{e1}$
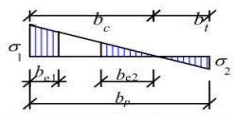	$\psi < 0$ $b_{eff} = \rho \cdot b_c = \rho b_p / (1-\psi)$ $b_{e1} = 0.4 \cdot b_{eff}; b_{e2} = 0.6 b_{eff}$

$\psi = \sigma_2 / \sigma_1$	1	$1 > \psi > 0$	0	$0 > \psi > -1$	-1	$-1 > \psi \geq -3$
Buckling factor k_σ	4.0	$8.2/(1.05+\psi)$	7.81	$7.81 - 6.29\psi + 9.78\psi^2$	23.9	$5.98(1-\psi)^2$

Table 2.Outstand compression elements

Table 3.6 – Outstand compression elements

Stress distribution (compression positive)	Effective width b_{eff}
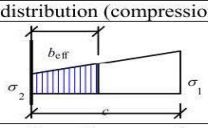	$1 > \psi \geq 0$ $b_{eff} = \rho \cdot c$
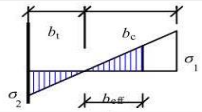	$\psi < 0$ $b_{eff} = \rho \cdot b_c = \rho c / (1-\psi)$

$\psi = \sigma_2 / \sigma_1$	1	0	-1	$1 \geq \psi \geq -3$
Buckling factor k_σ	0.43	0.57	0.85	$0.57 - 0.21\psi + 0.07\psi^2$

Stress distribution (compression positive)	Effective width b_{eff}
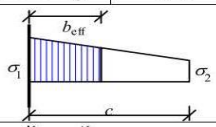	$1 > \psi \geq 0$ $b_{eff} = \rho \cdot c$
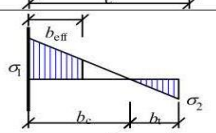	$\psi < 0$ $b_{eff} = \rho \cdot b_c = \rho c / (1-\psi)$

$\psi = \sigma_2 / \sigma_1$	1	$1 > \psi > 0$	0	$0 > \psi > -1$	-1
Buckling factor k_σ	0.43	$0.578/(\psi + 0.24)$	1.70	$1.7 - 5\psi + 17.1\psi^2$	23.8

B.3. The width reduction factor is :

if $\lambda_{P,c} \leq 0.748$

ρ : 1 = 1

if $\lambda_{P,c} > 0.748$

ρ : $(\lambda_{P,c} - 0.188) / \lambda_{P,c}^2 \leq 1$ = 1.000

So

ρ : = **1.000**

B.4. The effective width is :

c_{eff} : $\rho \cdot c_p$ = **18.800** mm

B.5. Effective area of the edge stiffener :

A_s : $t (b_{e2} + c_{eff})$ = **121.481** mm^2

2.4.2 Step 2 :

A. Effective width of the outstand compression flange

Use the initial effective cross section of the stiffener to determine the reduction factor, allowing for the effects of the continuous spring restraint.

The elastic buckling strees for the edge stiffener is,

$\sigma_{cr,s}$: $2 \sqrt{(K E I_s)} / A_s$

where :

K is the spring stiffness per unit length :

B. Spring stiffness per unit length

K : $E t^3 / (4 (1 - v^2) . 1 / (b_1^2 h_p + b_1^3 + 0.5 b_1 b_2 h_p k_f)$

with :

b_1 : distance from the web to the center of the effecive area of the stiffener in compression (upper flange)

b_1 : $b_{p1} - 0.5 b_{e2} t b_{e2} / [(b_{e2} + c_{eff}) t]$ = 62.229 mm

k_f : for bending about the y-y axis = 0

K : $E t^3 / (4 (1 - v^2) . 1 / (b_1^2 h_p + b_1^3 + 0.5 b_1 b_2 h_p k_f)$

= **0.653** N/mm

C. Effective second moment of area of the stiffener :

I_o mm^4	
$b_{e2} t^3 / 12$ =	35.79
$c_{eff}^3 t / 12$ =	1306.8
TOTAL	1342.6

A mm^2		y mm		$A y^2$ mm^4
$b_{e2} t$ =	77.113	$c_{eff}^2 / (2 (b_{e2} + c_{eff}))$ =	3.4331	908.8809908
$c_{eff} t$ =	44.368	$c_{eff} / 2 - c_{eff}^2 / (2 (b_{e2} + c_{eff}))$ =	5.9669	1579.654373
TOTAL				2488.535364

I_s : $\Sigma I_o + \Sigma A y^2$ = **3831.11** mm^4

D. The elastic critical buckling stress for the edge stiffener

so, the elastic critical buckling stress for the edge stiffener is,

$\sigma_{cr,s}$: $2 \sqrt{(K E I_s)} / A_s$ = **383.558** N/mm^2

E. Thickness reduction factor χ_d for the edge stiffener

The relative slenderness :

λ_d : $\sqrt{(f_{yb} / \sigma_{cr,s})}$ = 1.169

The reduction factor will be :

if $\lambda_d \leq 0.65$

χ_d : 1 = 1

if $0.65 < \lambda_d \leq 1.38$

χ_d : $1.47 - 0.723 \lambda_d$ = 0.625

if $\lambda_d \geq 1.38$

χ_d : $0.66 / \lambda_d$ = 0.565

So

χ_d : = **0.625**

2.4.3 Step 3 :

A. Iteration

As the reduction factor for buckling of the stiffener is $\chi_d < 1$, iterate to refine the value of the reduction factor for buckling of the stiffener.
The iterations are carried out based on modified values of ρ obtained using:

$\sigma_{com,Ed,I} = \chi_d f_{yb} / \gamma_{M0}$ and $\lambda_{p,red} = \lambda_p \sqrt{\chi_d}$

χ_d from previous iteration, continuing until $\chi_d \approx \chi_{d(n-1)}$ but $\chi_{d,n} \leq \chi_{d(n-1)}$

In this step:

$\chi_{d(n-1)}$	:		=	1
$\chi_{d,n}$	:		=	0.625
χ_d	:	$\chi_d \approx \chi_{d(n-1)}$ but $\chi_{d,n} \leq \chi_{d(n-1)}$	=	0.625

The iteration stops when the reduction factor χ converges.

Initial values (iteration 1) :			Final values (iteration n) :			
χ_d	=	0.625	$\chi_d = \chi_{d,n}$	=	0.601	mm
b_{e2}	=	32.675 mm	$b_{e2} = b_{e2,n}$	=	36.300	mm
c_{eff}	=	18.800 mm	$c_{eff} = c_{eff,n}$	=	18.800	mm

B. Final values

Final values of effective properies for flange and lipp in compression are :

χ_d	:		=	0.601	mm
b_{e2}	:		=	36.300	mm
c_{eff}	:		=	18.800	mm
b_{e1}	:		=	32.675	mm
t_{red}	:	$t \cdot \chi_d$	=	1.419	mm

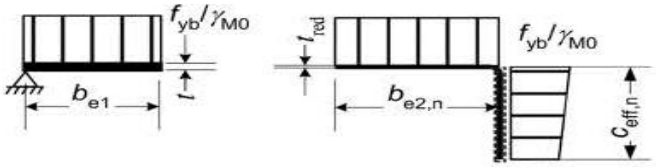

2.3. Effective section properties of the web

2.3.1 The position of the neutral axis with regard to the flange in compression :

h_c : $\Sigma A_1 Z / A_2$

Where the static moment

B mm			H mm			Z mm			$A_1 Z$ mm^3
c_p	=	18.8	t	=	2.36	$h_p - c_p / 2$	=	238.2	10568.4576
b_{p2}	=	72.6	t	=	2.36	h_p	=	247.6	42422.7936
h_p	=	247.6	t	=	2.36	$h_p / 2$	=	123.8	72340.7968
$c_{eff}\ \chi_d$	=	11.303	t	=	2.36	$c_{eff} / 2$	=	9.4	250.7362146
TOTAL									125582.7842

Total area

B mm			H mm			A_2 mm^2
c_p	=	18.8	t	=	2.36	44.368
b_{p2}	=	72.6	t	=	2.36	171.34
h_p	=	247.6	t	=	2.36	584.34
b_{e1}	=	32.675	t	=	2.36	77.113
$b_{e2}\ \chi_d$	=	21.824	t	=	2.36	51.504
$c_{eff}\ \chi_d$	=	11.303	t	=	2.36	26.674
TOTAL						955.33

The position of the neutral axis with regard to the flange in compression define as

h_c	:	$\Sigma A_1 Z / A_2$	=	131.455	mm

2.3.2 The stress ratio :

ψ : $(h_c - h_p) / c$ = -0.884

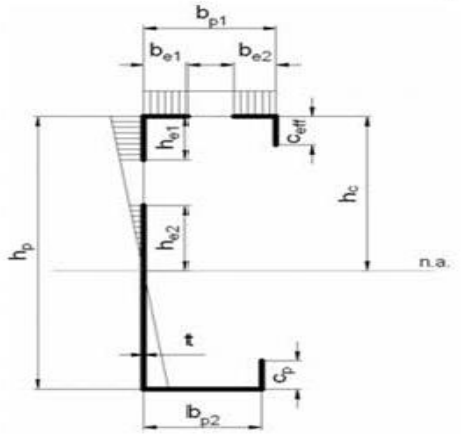

a. The buckling factor :

k_σ : $7.81 - 6.29\,\psi + 9.78\,\psi^2$ = 21.002

b. The relative slenderness :

$\lambda_{p,h}$: $\dfrac{h_p / t}{[28.4\,\varepsilon\sqrt{k_\sigma}]}$ = 1.204

c. The width reduction factor is :

ρ : $\dfrac{\lambda_{p,h} - 0.055\,(3 + \psi)}{\lambda_{p,h}}$ = 0.750

d. The effective width of the zone in compression of the web is :

h_{eff} : $\rho \,.\, h_c$ = 98.647 mm

e. Near the flange in compression :

h_{e1} : $0.4 \,.\, h_{eff}$ = 39.459 mm

f. Near the neutral axis :

h_{e2} : $0.6 \,.\, h_{eff}$ = 59.188 mm

g. The effective width of the web is :

Near the flange in compression :

h_1 : h_{e1} = 39.459 mm

Near the flange in tension :

h_2 : $h_p - (h_c - h_{e2})$ = 175.333 mm

2.4. Effective section properties

2.4.1 Effective cross-section area :

A_{eff} : ΣA_i

B mm			H mm			A_i mm²	
c_p	=	18.8	t	=	2.36	44.368	Tension / Bottom
b_{p2}	=	72.6	t	=	2.36	171.34	Tension / Bottom
h_1	=	39.459	t	=	2.36	93.123	
h_2	=	175.33	t	=	2.36	413.79	
b_{e1}	=	32.675	t	=	2.36	77.113	
b_{e2}	=	36.300	t χ_d	=	1.4188	51.504	
c_{eff}	=	18.800	t χ_d	=	1.4188	26.674	Compression / Top
TOTAL						877.9	

So from table above

A_{eff} : ΣA_i = 877.90 mm²

2.4.2 Position of the neutral axis with regard to the flange

Z_c : $\Sigma A Z / A_{eff}$

B mm			H mm			Z mm			A Z mm^3
c_p	=	18.8	t	=	2.36	$h_p - c_p / 2$	=	238.2	10568.4576
b_{p2}	=	72.6	t	=	2.36	h_p	=	247.6	42422.7936
h_2	=	175.33	t	=	2.36	$h_p - c_p / 2$	=	159.93	66178.30849
h_1	=	39.459	t	=	2.36	$h_1 / 2$	=	19.729	1837.2648
c_{eff}	=	18.800	t χ_d	=	1.4188	$c_{eff} / 2$	=	9.4	250.7362146
TOTAL									121257.5607

So from table above

Position of the neutral axis with regard to the flange in compression :

Z_c : = 138.122 mm

Position of the neutral axis with regard to the flange in tension :

Z_t : $h_p - z_c$ = 109.478 mm

2.4.3 Position of the centroid axis with regard to the web

B mm			H mm			Z mm			A Z mm^3
c_p	=	18.8	t	=	2.36	b_{p2}	=	72.6	3221.1168
b_{p2}	=	72.6	t	=	2.36	$b_{p2} / 2$	=	36.300	6219.4968
h_2	=	175.333	t	=	2.36	0	=	0	0
h_1	=	39.459	t	=	2.36	0	=	0	0
b_{e1}	=	32.675	t	=	2.36	$b_{e1} / 2$	=	16.337	1259.818013
b_{e2} χ_d	=	36.300	t	=	2.36	$b_{p1} - b_{e2} / 2$	=	54.45	72.6
c_{eff} χ_d	=	18.800	t	=	2.36	b_{p1}	=	72.600	3221.1168
TOTAL									10700.43161

Position of the neutral axis with regard to the flange in compression :

$y_{eff,z,com}$: $\Sigma B . T . Z / A_{eff}$ = 12.189 mm

Position of the centroid axis with regard to the web tension

$y_{eff,z,ten}$: $b_{p1} - y_{eff,z,com}$ = 60.411 mm

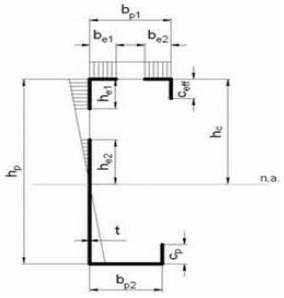

2.4.4 Second moment of area about strong axis :

$I_{eff,y}$: $I_0 + \Sigma A z^2$

Where for I_0

$I_{0,i}$ mm^4		
$h_1^3 t / 12$	=	12083
$h_2^3 t / 12$	=	1E+06
$b_{p2}^3 t / 12$	=	75256
$c_p^3 t / 12$	=	1306.8
$b_{e1}^3 t / 12$	=	6860.7
$b_{e2} (\chi_d t)^3 / 12$	=	8.6401
$c_{eff}^3 (\chi_d t) / 12$	=	785.64
TOTAL		1E+06

I_0 : $\Sigma I_{0,i}$ = 1156348.18 mm^4

And $\Sigma A y^2$

A mm^2			z mm			$A z^2$ mm^3
$c_p t$	=	44.368	$z_t - c_p /2$	=	100.08	444376
$b_{p2} t$	=	171.34	z_t	=	109.48	2E+06
$h_2 t$	=	413.79	$z_t - h_2 /2$	=	21.812	196858
$h_1 t$	=	93.123	$z_c - h_1 /2$	=	118.39	1E+06
$b_{e1} t$	=	77.113	z_c	=	138.12	1E+06
$b_{e2} (\chi_d t)$	=	46.36	z_c	=	138.12	884438
$c_{eff} (\chi_d t)$	=	26.674	$z_c - c_{eff} / 2$	=	128.72	441969
TOTAL						7E+06

$\Sigma A y^2$: = 6797589.992 mm^4

So

$I_{eff,y}$: $I_0 + \Sigma A y^2$ = 8.0E+06 mm^4

2.4.5 Effective section modulus :

With regard to the flange in compression

$W_{eff,y,c}$: $\frac{I_{eff,y}}{z_c}$ = 57586.5 mm^3

With regard to the flange in tension

$W_{eff,y,t}$: $\frac{I_{eff,y}}{z_t}$ = 72653 mm^3

2.4.6 Second moment of area about weak axis :

$I_{eff,z}$: $I_0 + \Sigma A y^2$

Where for I_0

$I_{0,i}$ mm^4		
$h_1 t^3 / 12$	=	43.221
$h_2 t^3 / 12$	=	192.05
$b_{p2} t^3 / 12$	=	79.523
$c_p t^3 / 12$	=	20.593
$b_{e1} t^3 / 12$	=	35.79
$b_{e2}^3 (\chi_d t) / 12$	=	5655.5
$c_{eff} (\chi_d t)^3 / 12$	=	4.4748
TOTAL		6031.1

I_0 : $\Sigma I_{0,i}$ = 6031.141297 mm^4

And $\Sigma A y^2$

A mm^2			y mm			$A y^2$
$c_p t$	=	44.368	b_{p2}	=	72.6	233853
$b_{p2} t$	=	171.34	$b_{p2} / 2$	=	36.300	225768
$h_2 t$	=	413.79	0	=	0	0
$h_1 t$	=	93.123	0	=	0	0
$b_{e1} t$	=	77.113	$b_{e1} / 2$	=	16.337	20582
$b_{e2} (\chi_d t)$	=	46.36	$b_{p1} - b_{e2} / 2$	=	54.45	137449
$c_{eff} (\chi_d t)$		26.674	b_{p1}	=	72.600	140593
TOTAL						758244

$\Sigma A y^2$: = 758244.0687 mm^4

So

$I_{eff,z}$: $I_0 + \Sigma A y^2$ = 7.6E+05 mm^4

2.4.7 Effective section modulus :

With regard to the flange in compression

$W_{eff,z,c}$: $\dfrac{I_{eff,z}}{y_c}$ = 12651.2 mm^3

With regard to the flange in tension

$W_{eff,z,t}$: $\dfrac{I_{eff,z}}{y_t}$ = 62704 mm^3

2.5. Summary for effective section properties (single section)

2.5.1 Drawing

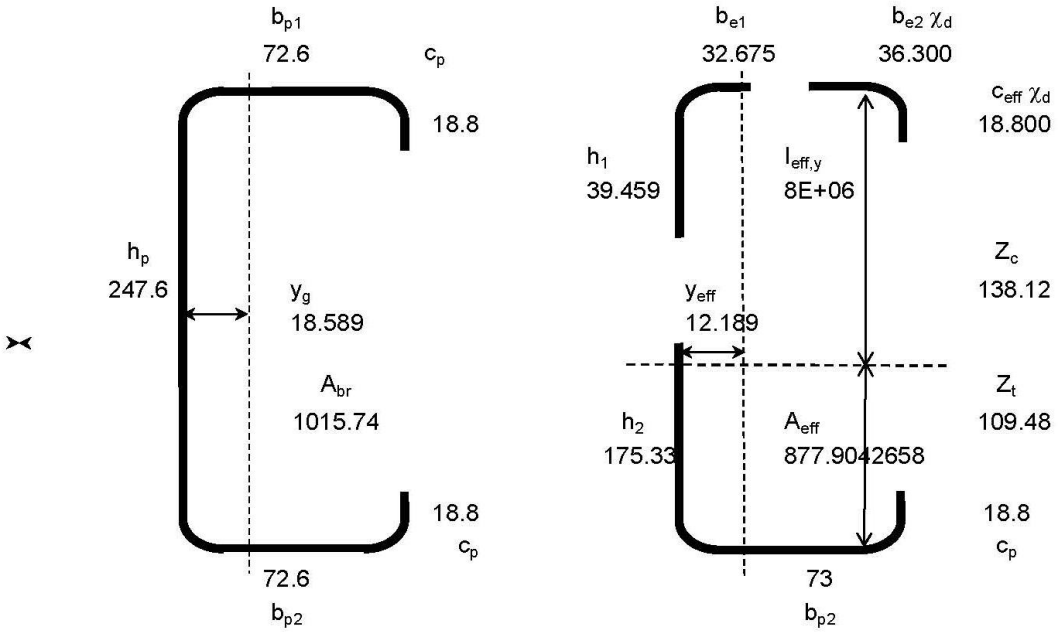

2.5.2 Property the Single Lipped Channel for bending

A_{eff}	:		=	877.90 mm^2
$I_{eff,y}$	:		=	7953938.2 mm^4
$W_{eff,y,c}$	:	Regard to the flange in compression	=	57586.48 mm^3
$W_{eff,y,t}$	:	Regard to the flange in tension	=	72653.05 mm^3
$W_{eff,y,min}$	:	min $W_{eff,y,c}$, $W_{eff,y,t}$	=	57586.48 mm^3
Z_c	:		=	138.12 mm
Z_t	:		=	109.48 mm
$M_{b,Rd}$	:	$W_{eff}\ f_{yb} / \gamma_{M0}$	=	30.18 kNm

2.5.3 Bending resistance (for doublelipped multiply by two)

γ_{M0}	:		=	1
$M_{c,Rd}$	:	$2\ W_{eff}\ f_{yb} / \gamma_{M0}$	=	60.351 Kn m

Buckling resistance of CFS Beamin bending

1. Data of lipped channel

Ref: Dubina ex 4.3-P295

Design of an unrestrained cold-formed steel beam in bending at the Ultimate Limit State (see Figure below). The beam has pinned end conditions and is composed of two thin-walled cold-formed steel back-to back lipped channel sections. The connection between the channels i assumed to be rigid.

Overall dimensions of beam and of the cross section

Type	:		=	C25024	
f_y	:	Basic yield strength	=	524	mPa
f_u	:	Ultimite stress	=	592.2	mPa
E_s	:	Modulus of elasticity	=	216963	mPa
v	:	Poisson's ratio	=	0.3	
G_s	:	Shear modulus $E_s / 2 (1 + v)$	=	83447.31	mPa
γ_{M1}	:	Partially safety factor	=	1	

2. Loading data

The dimensions of the section centre line are:

L	:	Span of beam	=	4000	mm

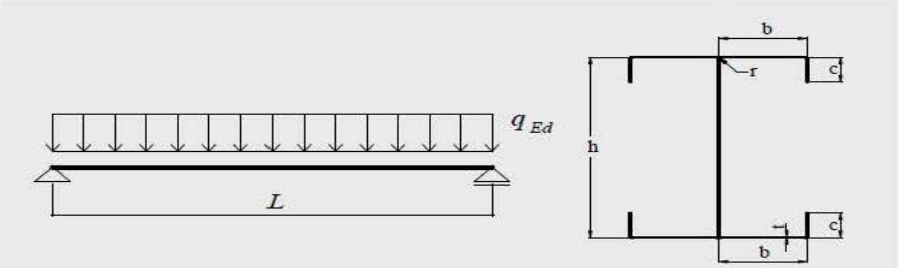

3 Properties of the DLC according to BS EN 1993-1-3:2006

3.1 Properties of the gross cross section

A	:	Area of gross cross section:	=	2.06E+03	mm^2
i_y	:	Radii of gyration:	=	1.01E+02	mm
i_z	:	Radii of gyration:	=	3.59E+01	mm
I_y	:	Second moment of area about strong axis y-y:	=	2.11E+07	mm^4
I_z	:	Second moment of area about weak axis z-z	=	2.66E+06	mm^4
I_w	:	Warping constant:	=	3.89E+10	mm^6
I_t	:	Torsion constant	=	2.09E+04	mm^4

3.2 Effective section properties of the cross section

a Inertia effective

The properties of effective cross section were calculated following the procedures for CFS effective section in bending is

$I_{eff,y}$	:	2	x	7.95E+06	=	1.59E+07	

Position of the neutral axis:

z_c	:	from the flange in compression	=	138.12	mm
z_t	:	from the flange in tension	=	109.48	mm

b Effective section modulus

With respect to the flange in compression:

$W_{eff,y,c}$	:	$I_{eff,y} / z_c$	=	1.15E+05	mm^3

With respect to the flange in tension:

$W_{eff,y,t}$	:	$I_{eff,y} / z_t$	=	1.45E+05	mm^3
$W_{eff,y\ min}$	:	min of $W_{eff,y,c}$ and $W_{eff,y,t}$	=	1.15E+05	mm^3

4. Check of bending resistance at buckling

a. Basic requirement:

$M_{b,Rd}$: $\chi_{LT} W_{eff,y} f_{yb} / \gamma_{M1}$

b. Determination of the reduction factor χ_{LT}

Basic requirement:

χ_{LT} : $1 / (\Phi_{LT} + (\Phi_{LT}^2 - \lambda_{LT}^2)^{0.5}) \leq 1$

Where

Φ_{LT} : $0.5 [1 + \alpha_{LT} (\lambda_{LT} - 0.2) + \lambda_{LT}^2]$

Coefficients C_1, C_2 and C_3 for beams with end moments
Boissonnade et al (2006).

Loading and support conditions	Diagram of moments	k_z	C_1	C_3	
				$\psi_f \leq 0$	$\psi_f > 0$
	$\Psi = +1$	1.0	1.00	1.000	
		0.5	1.05	1.019	
	$\Psi = +3/4$	1.0	1.14	1.000	
		0.5	1.19	1.017	
	$\Psi = +1/2$	1.0	1.31	1.000	
		0.5	1.37	1.000	
	$\Psi = +1/4$	1.0	1.52	1.000	
		0.5	1.60	1.000	
	$\Psi = 0$	1.0	1.77	1.000	
		0.5	1.86	1.000	
	$\Psi = -1/4$	1.0	2.06	1.000	0.850
		0.5	2.15	1.000	0.650
	$\Psi = -1/2$	1.0	2.35	1.000	$1.3-1.2\psi_f$
		0.5	2.42	0.950	$0.77\psi_f$
	$\Psi = -3/4$	1.0	2.60	1.000	$0.55\psi_f$
		0.5	2.45	0.850	$0.35\psi_f$
	$\Psi = -1$	1.0	2.60	$-\psi_f$	$-\psi_f$
		0.5	2.45	$-0.125-0.7\psi_f$	$-0.125-0.7\psi_f$

- In beams subjected to end moments, by definition $C_2 z_g = 0$;
- $\psi_f = \dfrac{I_{fc} - I_{ft}}{I_{fc} + I_{ft}}$, where I_{fc} and I_{ft} are the second moments of area of the compression and tension flanges respectively, relative to the weak axis of the section ($z-z$ axis);
- C_1 must be divided by 1.05 when $\dfrac{\pi}{k_w L}\sqrt{\dfrac{EI_w}{GI_T}} \leq 1.0$, but $C_1 \geq 1.0$.

Coefficients C_1, C_2 and C_3 for beams with transverse loads
Boissonnade et al (2006).

Loading and support conditions	Diagram of moments	k_z	C_1	C_2	C_3
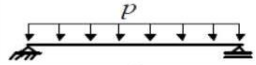	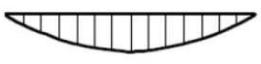	1.0	1.127	0.454	0.525
		0.5	0.97	0.36	0.478
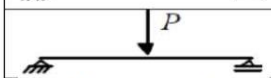	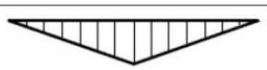	1.0	1.348	0.630	0.411
		0.5	1.05	0.48	0.338
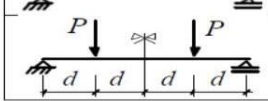	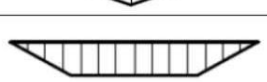	1.0	1.04	0.42	0.562
		0.5	0.95	0.31	0.539

kz is effective length factor related to rotations at the end sections about the weak axis z-z, 0.5 if restrained deformations, 1.0 free deformations, 0.7 in the case of free deformations at one & restrained deformations at the other. In most practical situations restraint is only partial, conservatively value of kz and kw = 1.0 may be adopted

k_z	:	Free deformation	=	1
C_1	:	for a simply supported beam under uniform loading		
	:		=	1.04
M_{cr}	:	The elastic critical moment for lateral-torsional buckling		
	:	$C_1 \pi^2 E_s I_z / L^2 (I_w / I_z + L^2 G_s I_t / (\pi^2 E_s I_z))^{0.5}$		
	:		=	517.63 Kn m

The non-dimensional slenderness is

λ_{LT}	:	$(W_{eff,ymin} f_y / M_{cr})^{0.5}$	=	0.341

Lateral-torsional buckling

Imperfection factor α for buckling curve

Buckling curve	a_0	a	b	c	d
α	0.13	0.21	0.34	0.49	0.76

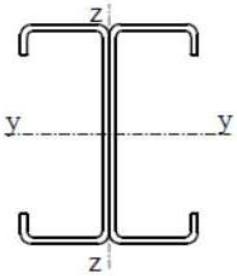

Axis	Buckling curve
y-y	a
z-z	b

In this case from table and figure above for buckling in z-z axis the buckling curve "b" is taken.

α_{LT}	:	Imperfection factor lateral buckling	=	0.34
Φ_{LT}	:	$0.5 [1 + \alpha_{LT} (\lambda_{LT} - 0.2) + \lambda_{LT}^2]$	=	0.582
χ_{LT}	:	$1 / (\Phi_{LT} + (\Phi_{LT}^2 - \lambda_{LT}^2)^{0.5}) \leq 1$	=	0.949

c. Design bending moment resistance for double lipped channel

$M_{b,Rd}$	:	$\chi_{LT} W_{eff,y\,min} f_y / \gamma_{M1}$	=	57.25 kN m

SHEAR BUCKLING RESISTANCE

1. Shear resistance beam lipped channel single section

1.1. General

According to BSEN 1993 1-3 δ6.1.5, for cold-formed the design shear resistance $V_{b,Rd}$ should be determined with equation:

$V_{b,Rd}$: $\dfrac{(h_w / \sin\phi)\, t\, f_{bv}}{\gamma_{M0}}$ BSEN 1993 1-3 δ6.1.5.

f_{bv} : The shear strength considering buckling

h_w : The web height between the midlines of the flanges

ϕ : The slope of the web relative to the flanges

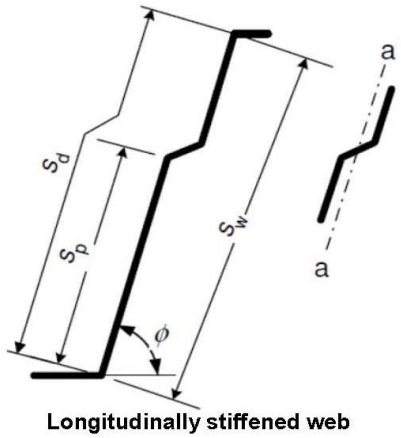

Longitudinally stiffened web

Shear buckling strength f_{bv}

Relative web slenderness	Web without stiffening at the support	Web with stiffening at the support [1]
$\bar{\lambda}_w \le 0{,}83$	$0{,}58 f_{yb}$	$0{,}58 f_{yb}$
$0{,}83 < \bar{\lambda}_w < 1{,}40$	$0{,}48 f_{yb} / \bar{\lambda}_w$	$0{,}48 f_{yb} / \bar{\lambda}_w$
$\bar{\lambda}_w \ge 1{,}40$	$0{,}67 f_{yb} / \bar{\lambda}_w^2$	$0{,}48 f_{yb} / \bar{\lambda}_w$

[1] Stiffening at the support, such as cleats, arranged to prevent distortion of the web and designed to resist the support reaction.

The relative slenderness λ_w in case without longitudinal stiffness is:

λ_w : $0.346\, s_w / t \sqrt{[\, f_{yb} / E \,]}$

The shear resistance can be better improved when the value of Sw changed from the total depth to the effective depth in shear resistance.

1.2. Data

Stiffening at the support	:		=	Yes	
h_b	:		=	250	mm
t_{nom}	:	$t_{fb,0}$	=	2.4	mm
t	:	Core thickness t_{fb}	=	2.36	mm
s_w	:	$h_b - t_{nom}$	=	206.2	mm
f_{yb}	:	$f_{y,beam}$	=	524	Mpa
E_s	:	Modulus of elasticity	=	216963	Mpa
The web height between the midlines of the flanges					
h_w	:	$h_b - t_{nom}$	=	247.6	mm
ϕ	:		=	90	degree
γ_{M0}	:	Partial strength	=	1	

1.3 Buckling Shear resistance $V_{b,Rd}$

The relative slenderness λ_w in case without longitudinal stiffness is:

λ_w : $0.346\, s_w / t \sqrt{[\, f_{yb} / E_s \,]}$ = 1.486

For web without stiffening at the support

f_{bv}	:	$0.58\, f_{yb} / \lambda_w$	if $\lambda_w \le 0.83$	=	204.5661
	:	$0.48\, f_{yb} / \lambda_w$	if $0.83 < \lambda_w < 1.40$	=	169.2961
	:	$0.67\, f_{yb} / \lambda_w^2$	if $\lambda_w \ge 1.40$	=	159.0578

For web with stiffening at the support

f_{bv}	:	$0.58\, f_{yb} / \lambda_w$	if $\lambda_w \le 0.83$	=	204.5661
	:	$0.48\, f_{yb} / \lambda_w$	if $0.83 < \lambda_w < 1.40$	=	169.2961
	:	$0.48\, f_{yb} / \lambda_w$	if $\lambda_w \ge 1.40$	=	169.2961

So

f_{bv} : = 169.2961 N/mm^2

Shear resistance for single section 169.3

$V_{b,Rd}$: $\dfrac{(h_w / \sin\phi)\, t\, f_{bv}}{\gamma_{M0}}$ $V_{b,Rd}$ = 98.926 KN

2.1 Buckling Shear resistance $V_{b,Rd}$ (using post-critic method)

web slenderness

$$\lambda_w = \frac{d/t_w}{37.4\varepsilon\sqrt{k_t}} = 1.7$$

value of the simple post-critic resistance

$$\tau_{ba} = \left[1 - 0.625\left(\lambda_w - 0.8\right)\right]\left(\frac{f_{yb}}{\sqrt{3}}\right) = 226.9 \text{ N/mm}^2$$

Shear buckling resistance

$$V_{ba,Rd} = \frac{dt_w\tau_{ba}}{\gamma_a} = 133.5 \text{ kN}$$

3.1 Plastic vertical shear resistance

Shear area

$$A_v = A - 2bt + t\left(t + 2r\right) \ge \eta h_w t = 564.5 \text{ mm}^2$$

$$\eta h_w t = 523.8 \text{ mm}^2$$

$$V_{pla,Rd} = \frac{A_v\left(f_{yb}/\sqrt{3}\right)}{\gamma_{mo}} = 170.8 \text{ kN}$$

1.3 Buckling Shear resistance $V_{b,Rd}$

The relative slenderness λ_w in case without longitudinal stiffness is:

λ_w : $0.346\, s_w / t \sqrt{[\, f_{yb} / E_s \,]}$ = 1.486

For web without stiffening at the support

f_{bv}	:	$0.58\, f_{yb} / \lambda_w$	if $\lambda_w \le 0.83$	=	204.5661
	:	$0.48\, f_{yb} / \lambda_w$	if $0.83 < \lambda_w < 1.40$	=	169.2961
	:	$0.67\, f_{yb} / \lambda_w^2$	if $\lambda_w \ge 1.40$	=	159.0578

For web with stiffening at the support

f_{bv}	:	$0.58\, f_{yb} / \lambda_w$	if $\lambda_w \le 0.83$	=	204.5661
	:	$0.48\, f_{yb} / \lambda_w$	if $0.83 < \lambda_w < 1.40$	=	169.2961
	:	$0.48\, f_{yb} / \lambda_w$	if $\lambda_w \ge 1.40$	=	169.2961

So

f_{bv} : = 169.2961 N/mm^2

Shear resistance for single section 169.3

$V_{b,Rd}$: $\dfrac{(h_w / \sin\phi)\, t\, f_{bv}}{\gamma_{M0}}$ $V_{b,Rd}$ = 98.926 KN

2.1 Buckling Shear resistance $V_{b,Rd}$ (using post-critic method)

web slenderness

$$\lambda_w = \frac{d/t_w}{37.4\varepsilon\sqrt{k_t}} = 1.7$$

value of the simple post-critic resistance

$$\tau_{ba} = \left[1 - 0.625\left(\lambda_w - 0.8\right)\right]\left(\frac{f_{yb}}{\sqrt{3}}\right) = 226.9 \text{ N/mm}^2$$

Shear buckling resistance

$$V_{ba,Rd} = \frac{dt_w\tau_{ba}}{\gamma_a} = 133.5 \text{ kN}$$

3.1 Plastic vertical shear resistance

Shear area

$$A_v = A - 2bt + t\left(t + 2r\right) \ge \eta h_w t = 564.5 \text{ mm}^2$$

$$\eta h_w t = 523.8 \text{ mm}^2$$

$$V_{pla,Rd} = \frac{A_v\left(f_{yb}/\sqrt{3}\right)}{\gamma_{mo}} = 170.8 \text{ kN}$$

APPENDIX C

Design Calculation of Composite beam
Example (CBS-CS-BB-250-12-C75+Ø12) (CBS1)

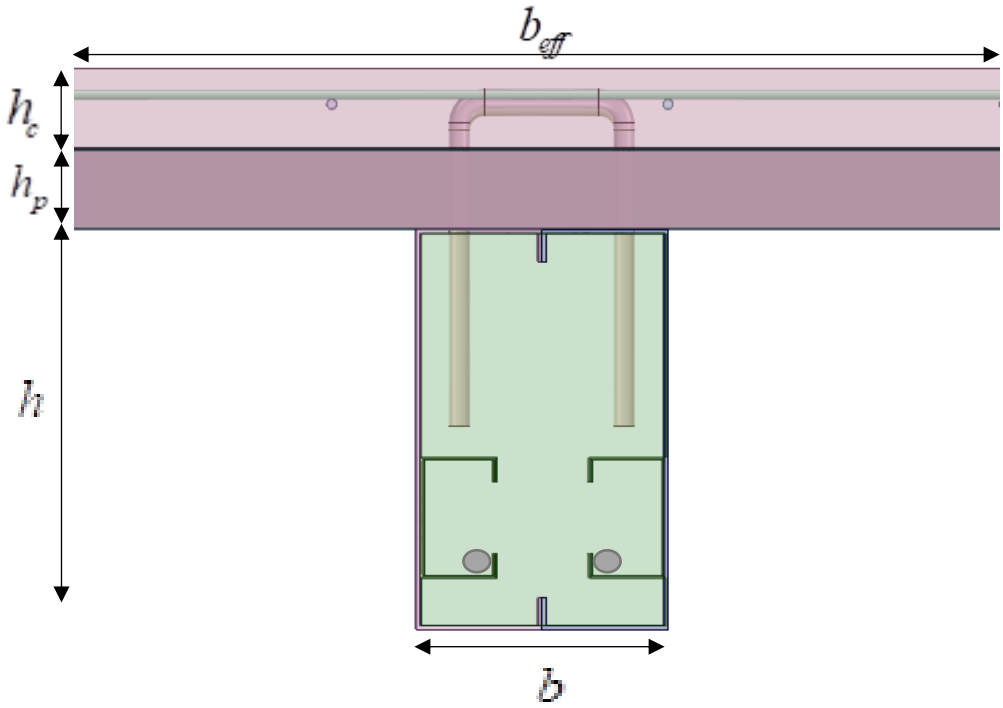

INPUT

Beam data

h	Total height = 250 mm
b	Width of flange = 150 mm
c	Edge fold = 20 mm
r	Internal radius = 5 mm
t	Nominal thickness = 2.4 mm
t_{nom}	Steel core thickness = 2.36 mm
f_{yb}	Yield strength = 524 N/mm^2

E_s Modulus of elasticity = 216963 N/mm^2

ϕ Angle = 90°

A_{eff} Section area = 1724.6 mm^2

I_{eff} Second moment of area = 15.8E+06 mm^4

W_{eff} Elastic section modulus = 11.3 E+4 mm^3

Slab data

L Length = 4000 mm

b_{eff} Width = 750 mm

h_c Depth of concrete flange = 50 mm

h_p Depth of steel sheeting height = 50 mm

d' Concrete cover = 25 mm

f_{ck} Compressive strength of concrete = 55.6 N/mm^2

E_c Modulus of elasticity = 35056 N/mm^2

$M_{pl,steel}$ Moment resistance of the CFS beam = 57.3 kNm

Shear connector data

d Diameter = 12 mm

f_{yr} Yield strength = 656.6 N/mm^2

$P_{Rd,s}$ Shear resistance of shear connector = 50.7 kN

n Number of shear connectors = 26

Reinforcement data

d Diameter = 12 mm

f_{yr} Yield strength = 656.6 N/mm^2

n Number of rebars = 2

A_r Section area = 113.0 mm^2

Partial safety factors

γ_{mo} Safety factor = 1.0

γ_a Safety factor of steel = 1.05

γ_v Safety factor = 1.25

γ_c Safety factor of concrete = 1.5

COMPOSITE DESIGN

1. Compressive resistance of slab R_c

$$R_c = \frac{0.85 f_{ck} b_{eff} h_c}{\gamma_c} = 1182.2 \text{ kN}$$

2. Tensile resistance of steel section R_s

$$R_s = F_s + F_r + F_{st}$$

$$R_s = A_s . f_{yb} + A_r . f_{yr} + A_{st} . f_{yst} = 1384.6 \text{ kN}$$

3. Moment resistance with full shear connection $M_{pI,Rd}$

Since $R_c < R_s$ the plastic neutral axis (P.N.A.) lies in the steel flange, therefore the moment resistance of the composite beam is:

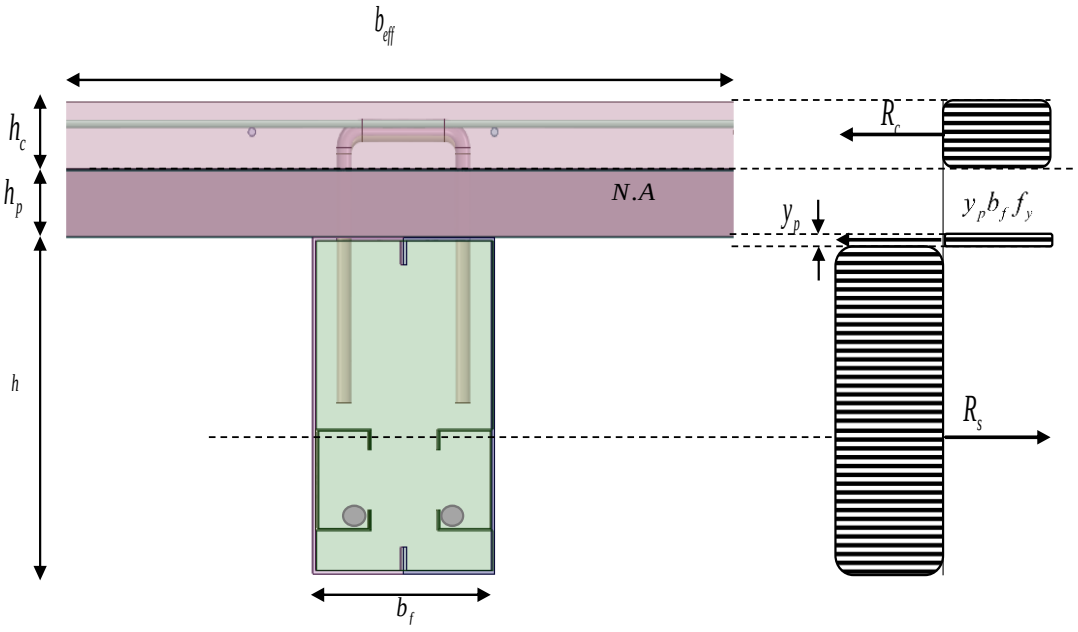

$$M_{pI,Rd} = R_c\left(\frac{h_c}{2} + h_p\right) + R_s\frac{h}{2} - \frac{\left(R_s - R_c\right)^2}{4b_f p_y} = 236.8 \text{ kNm}$$

The plastic neutral axis depth is:

$$y_p = \frac{R_s - R_c}{2b_f p_y} = 56 \text{ mm}$$

4. Shear connector resistance R_Q

The shear resistance of shear connector was obtained experimentally from push-out test, and it had a value of 50.7 kN per connector. Hence the total shear connector resistance is:

$$R_Q = nP_{Rd} = 1319.7 \text{ kN}$$

5. Degree of shear connection η

There is a minimum degree of shear connection which for beams with a span equal or less than 5 m is 0.4.

$$\eta = \frac{R_Q}{R}$$

R is the bending resistance of the critical cross-section which is limited either by the resistance of the concrete slab (R_c) or by the resistance of the steel beam(R_s).

$\eta = 1.116$

The degree of shear connection cannot be higher than 1 and less than a minimum equal to 0.4.

$\eta_p = 2 - \eta$ = 0.88

6. Moment resistance with partial shear connection $M_{c,Rd}$

Using the linear interaction method, the moment resistance of a composite beam is obtained as follows:

$M_{c,Rd} = M_{pI,steel} + \eta\left(M_{pI,Rd} - M_{pI,steel}\right)$ = 217 kNm

This resistance is per half of the composite specimen

$$\frac{M_{u,\exp}}{2M_{c,Rd}} = \frac{443.1}{2*217.0} = 1.02$$

LIST OF PUBLICATIONS

Title	Journal	Status	Date	Indexing
Behaviour of Boxed Cold-Formed Steel as Composite Beam with Rebar as Shear Connector	Advances and Challenges in Structural Engineering	Published	28.10.2018	Book Chapter
Experimental Study on Flexural Behaviour of Partially Encased Cold-Formed Steel Composite Beams Using Rebar as Shear Connector	IOP Conf. Series: Materials Science and Engineering 513	Published	30.04.2019	Scopus
Performance Evaluation of Pre-Fabricated Footing Using Cold-Formed Steel of Lipped C-Channel Section	Arabian Journal for Science and Engineering	Published	05.08.2019	WoS (Q3)
Behaviour of Rebar Shear Connector in A Push Test for Composite Beam with Cold-Formed Steel Section	IOP Conf. Series: Materials Science and Engineering 620	Published	19.11.2019	Scopus
Experimental and Analytical Study on Composite Connection with Cold-Formed Steel of Double Channel Sections	IOP Conf. Series: Materials Science and Engineering 620	Published	19.11.2019	Scopus
Bending Experiment on A Novel Configuration of Composite System Using Rebar as Shear Connectors with Partially Encased Cold-Formed Steel Built-Up Beams	Materials Today: Proceedings	Published	15.05.2020	Scopus
Influence of Seat Angles on the Behaviour of Cold-Formed Steel-Concrete Composite Joints	Journal of Constructional Steel Research	Accepted	29.06.2020	WoS (Q2)
Experimental study on composite connection with double lipped C- Sections	IOP Conf. Series: Materials Science and Engineering 849	Published	01.05.2020	Scopus
Behaviour of rectangular gusset plate with angle cleat connections for cold-formed steel section	IOP Conf. Series: Materials Science and Engineering 849	Published	01.05.2020	Scopus
Behaviour of Composite Beam Arranged as Boxed-Section With C- Channel of Cold-Formed Steel of Lipped Section	IOP Conf. Series: Materials Science and Engineering 849	Published	01.05.2020	Scopus